

CHAPTER 5. MOLECULAR MODELING

In chemistry (chemical synthesis), reactions are generally under thermodynamic control. The components are mixed, and the final product(s) is (are) the one with the most stable ground state. This requires that all reactions be reversible under the reaction conditions, so that an inherently dynamic system can find the lowest energy structure. Therefore, newly formed bonds must be relatively weak, so they can break and reform repeatedly under the reaction conditions until the thermodynamic sink (the lowest energy structure) is found. This would be supramolecular chemistry in its purest form. A key in supramolecular assembly is to have some weak, reversibly formed bonds. In this way, mistakes can be corrected.^{1,2} Some how, some of the ideas/concepts/hypotheses put forward to explain the oxidative coupling products as discussed in Chapter 4, could possibly be directed along this line. To test these ideas, some of the calculations are performed in gas phase and reported below. These calculations include Bond Dissociation Energy (BDE) and Ionization Potential (IP) of some stilbenoids, spin density computation for some stilbenoid radical and radical cation species, modeling of various stilbene pairs to understand the type of interactions involved as well as their stabilities and finally, the impact of metal ion Ag^+ on stilbene pair. Before proceeding with the above calculations, some reminders on general notions in physical chemistry, quantum mechanics concept and some general presentation of chemical interactions are provided.

5.1. Reminders on some general notions in physical chemistry

5.1.1. Enthalpy

The change in enthalpy, ΔH can be defined as the change in heat between two different compositions of a group of molecules at constant pressure if no work is done.^{1,3,4} In a chemical reaction, a change in heat is mainly accompanied by a change in bonding between two states (both intramolecular and intermolecular interactions). Thus, bond strengths (*i.e.*, strains on bonds, angles, torsion angles, non-bonding atoms) will give a good clue on the change of enthalpy and stability. During a reaction each of these strains may be modified, either reinforced or weakened, making the system of molecules more or less stable. Reactions are classified as either exothermic ($\Delta H < 0$) or endothermic ($\Delta H > 0$) on the basis of whether they release or absorb heat.

5.1.2. Entropy

Disorder of a system is given by its entropy S . Entropy can be associated with molecular and atomic movements or degrees of freedom (translational, rotational and vibrational).^{1,3,4} The more conformations a molecule can have, the more disordered it is. Thus, the entropy becomes more favorable to reaction conversion.

5.1.3. Gibbs free energy

The change in Gibbs free energy, ΔG° during a transformation is the difference in stability between two different compositions of a group of molecules (reactants and products) at constant pressure and standard states.^{1,3,4} Gibbs free energy

also can be considered as a driving force for a spontaneous change in composition. Eq 5.1 gives the correlation between the equilibrium constant, K_{eq} and the free energy change, ΔG° for any chemical process. At the equilibrium for a simple transformation that interconvert A and B ($A \leftrightarrow B$), K_{eq} is the ratio between species A and B (Eq 5.2).

$$\ln K_{eq} = -\Delta G^\circ / RT \quad \text{Eq 5.1}$$

$$K_{eq} = [B]/[A] \quad \text{Eq 5.2}$$

Gibbs free energy of a system is given by Eq 5.3, which incorporates the enthalpy (ΔH°) and the entropy (ΔS°) variations.

$$\Delta G^\circ = \Delta H^\circ - T\Delta S^\circ \quad \text{Eq 5.3}$$

Changes in temperature affect the free energy between A and B, and therefore the equilibrium constant. Based on the Eq 5.3, ΔG° is negative for any reaction when ΔH° is negative and ΔS° is positive. A reaction for which ΔG° is negative is thermodynamically favorable or spontaneous. On the other hand, ΔG° is positive for non spontaneous reaction. Strictly speaking ΔG° is negative when ΔH° is lower than $T\Delta S^\circ$. Nonetheless, the general trend for a spontaneous chemical process corresponds to reactions for which ΔH° is negative (*i.e.*, exothermic reaction) and ΔS° is positive (*i.e.*, reaction which increases disorder). The entropy becomes important especially when differences in ΔH° are small. Entropy also plays an important role in molecular recognition and solvation phenomena.

5.2. Quantum mechanics

The motion of electrons and other sub-nano particles cannot be described by classical mechanics (*i.e.*, Newton mechanics). Quantum Mechanics has been developed to study such motions.^{1,3,4} One of the central concepts of quantum

mechanics is the wave-particle duality, which states that electrons show wave-like as well as particle-like behavior.

5.2.1. The Schrödinger equation

All the information regarding electrons can be obtained from their wavefunctions. This can be done by solving the Schrödinger equation (eq. 5.4).^{1,3,4} All the forces on the system are collected in the Hamiltonian operator, \mathcal{H} . The forces are a function of the various positions of the electrons and nuclei. An operator indicates a mathematical operation (such as differentiation, multiplication, etc.) that acts on a function. Eq 5.4 shows an operator (\mathcal{H}) acting on a wave function (ψ) and giving back the same function (ψ) multiplied by a constant (E) which corresponds to the energy of the system.

$$\mathcal{H}\psi = E\psi \quad \text{Eq 5.4}$$

To solve this equation and find the wavefunction and the energy, the forces operating on the system (\mathcal{H}) need to be known. The Hamiltonian operator \mathcal{H} can be divided broken into two operators (T et V) (eq 5.5) corresponding to two contributions, a) kinetic energy and b) potential energy made of attraction-repulsion forces between particles:

$$\begin{aligned} \mathcal{H} &= T + V && \text{Eq. 5.5} \\ &= \text{Kinetic energy of nuclei} + \text{kinetic energy of electrons} + \text{nuclear-} \\ &\quad \text{nuclear repulsions} + \text{electron-electron repulsion} + \text{nuclear-} \\ &\quad \text{electron attraction.} \end{aligned}$$

5.2.2. Calculation methods - Solving the Schrödinger equation for complex systems

For pure two-body systems, like the hydrogen atom which contains one electron, it is possible to solve the Schrödinger equation analytically. For systems with few electrons, such as helium, the "many-electron" problem can be solved more or less exactly (at present the non-relativistic ground state energy of helium is known with fifteen significant figures).^{1,3,4} More general many-electron systems (molecules and a majority of the elements in the periodic table) cannot be treated with such precision, however. To study such systems we have to take advantages of the advent of high powered computers and to rely on some approximation methods.

5.2.2.1. Born-Oppenheimer's approximation and methods of calculation

The mass of a nucleus is more than a thousand times the mass of an electron. Due to that, nuclei move far more slowly than electrons. The electrons "see" the heavy, slow-moving nuclei as almost stationary point charges. From another point of view, the nuclei "see" the fast-moving electrons as a three-dimensional cloud of charges.^{1,3,4}

Based on Born-Oppenheimer's approximation, two types of calculation methods were developed, molecular mechanics and quantum chemistry. The former consists in the nuclei motion study. In this case nuclei and bonds are described by balls and springs, respectively, and the motion is studied by classical mechanics. Molecular mechanics is well-adapted to study large molecular systems (*e.g.*, proteins, polymers). Yet, since electrons are not explicitly described in equations, these methods cannot provide reliable results concerning chemical reactivity. The latter method type (quantum chemistry) explicitly treats the electron motion, and assumes a fixed

configuration of nuclei. The electronic Schrödinger equation is therefore solved by omitting the nuclear kinetic energy term. The equation is solved for different fixed nuclear configurations until the minimum electronic energy is obtained, which corresponds to the equilibrium geometry of the molecule.

5.2.3. Electron spin and molecular orbitals

To solve the Schrödinger equation, a mathematical expression of the total wavefunction of the molecule is required.^{1,3,4} This expression is a combination of one-electron molecular spinorbitals $\psi_a(1)$, $\psi_b(2)$, etc. The mathematical expression can be written as a Slater determinant. Let us remind that electrons can have either an up (\uparrow) or a down (\downarrow) spin. A molecular orbital is the product (so-called spinorbital) of a spatial molecular orbital and a spin function (\uparrow or \downarrow).

5.2.4. The Pauli exclusion principle

For electrons in a single atom, the Pauli exclusion principle states that no two electrons can have the same four quantum numbers, that is, if n , l , and m_l are the same, m_s must be different such that the electrons have opposite spins.^{1,3,4} More generally the Pauli principle states that no two identical fermions may occupy the same quantum state simultaneously. A mathematical statement of this principle is that the total wave function needs to be anti-symmetric, *i.e.*, if two identical fermions are interchanged the sign of the total wave function is changed.

5.2.5. Hartree–Fock method

One widely used approximation method to solve the electronic Schrödinger equation is the Hartree-Fock method. It is based on the rather natural approximation that each electron moves in the field created by the nucleus plus the average field potential of all the other electrons, rather considering instantaneous repulsion between individual electrons.^{1,3,4,5a} This assumption leads to the *independent-particle model*, which essentially reduces the many-electron problem to the problem of solving a number of coupled single-electron equations.

The Hartree-Fock (HF) approximation is a relatively fast method, which provides a first approximation for a wide range of atomic systems. Nonetheless this method fails to simulate various molecular systems, as compared to experimental data. The HF method does not account for all electron correlation contributions. Actually it just includes the correlation between electrons of parallel spin, which is called the exchange contribution. This basic correlation prevents two parallel-spin electrons from being found at the same point in space and is often called Fermi correlation.

The HF approximation does not take into account Coulomb correlations, leading to a total electronic energy different from the exact solution of the non-relativistic Schrödinger equation within the Born-Oppenheimer approximation. Therefore the HF limit is always above this exact energy. The difference is the so-called correlation energy, which mainly includes the correlation between electrons with opposite spin.

5.2.5.1. Self-consistent field (SCF) theory

To solve the Schrödinger equation (*i.e.* to obtain ψ) one needs the Hamiltonian, but the Hamiltonian operator \mathbf{H} depends on ψ . So an iterative calculation

is performed in a self-consistent field (SCF) way.^{1,3,4,5a} The ψ 's need to be guessed, the integrals and \hat{H} are evaluated, Hartree-Fock equation is solved and finally the E_{tot} value is obtained. The new ψ 's that are generated by this procedure are used and the entire process is repeated until the calculation converges to the lowest energy, *i.e.* when the new cycle leaves the energy unchanged. The orbitals are then said to be self-consistent with the field generated by the electrons, which referred to as self-consistent field (SCF) calculations.

5.2.6. Basis sets

Basis sets are a series of functions that are used by the computational chemistry to give a mathematical expression of spinorbitals. Actually spinorbitals are linear combinations of atomic orbitals and basis sets, which give an expression of atomic orbital.^{1,3,4,5a} There exists a wide variety of basis sets, and the choice of the proper basis set for a calculation is an important decision that the computational chemist needs to make. The most popular basis sets were developed by Pople and co-workers and correspond to a linear combination of Gaussian functions^{5b}. Depending on the number of Gaussian functions used the basis sets are named 3-21G, 6-31G, 6-311G and *etc.* For this work, two basis sets were used, both were 6-31 but including more or less polarized and diffuse functions.

5.2.6.1. Polarized basis sets

Normally, the location of the electrons is described in terms of their electron configuration. For example, for hydrogen and for carbon the configuration is described as $1s^2$ and $1s^2 2s^2 2p^2$, respectively. This accounts for one and six electrons, respectively. The corresponding orbitals are symmetric as regards to the nucleus,

naturally, but also when they are described by a Gaussian function. Such a description does not explicitly and accurately take into account polarization effects, which can be crucial in some chemical problems. To give a better mathematical description *p* or *d* orbitals are used to describe hydrogen or carbon atoms, respectively.^{1,3,4,5a} As can be seen in Figure 5.1 below, combining a *p* orbital to an *s* orbital for hydrogen atoms artificially polarizes the subsequent orbital. Such a mathematical approach allows more flexibility to describe the electronic structure.

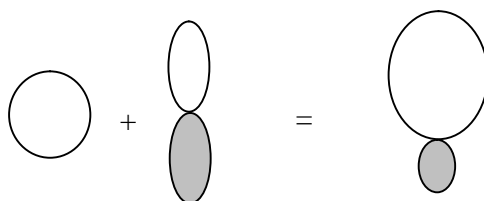


Figure 5.1: Simplified diagram of the linear combination of *s* and *p* orbitals.

In other words, polarization gives a more accurate description of where the electron is and where the electron can go. A polarized basis set is indicated by a \tilde{o}^*o in some places, or by the orbital name in others. For example, we can have a 3-21G* basis set or a 3-21G(d) basis set. Both refer to the same basis set.

5.2.6.2. Diffuse basis sets

Electrons are typically found close to the nucleus of the atom. We are interested in determining the probability of where electrons are, and that probability is highest near the nucleus. It then holds that, as the distance from the nucleus gets larger (bigger atomic radius), the probability of finding the electron gets lower. At large distances from the nucleus, calculations can be stopped, because typically electrons would not be formed there.^{1,3,4,5a} The Gaussian functions classically give a reliable

estimation of this behavior. Indeed these functions are at maximum on the nucleus and quickly decrease with the distance from the nucleus. For some systems, however, especially anions and atoms in the excited states, we use diffuse basis sets to extend the distance from the nucleus at which we are looking for electrons. This is mathematically obtained by adding “diffuse” or flatter Gaussian functions, *i.e.* lower value at the nucleus but slower decrease with distance (Figure 5.2). These basis sets are indicated by a “+” symbol, such as 3-21+G. A basis set like 6-312+G(d) would be a polarized diffuse split-valence basis set.

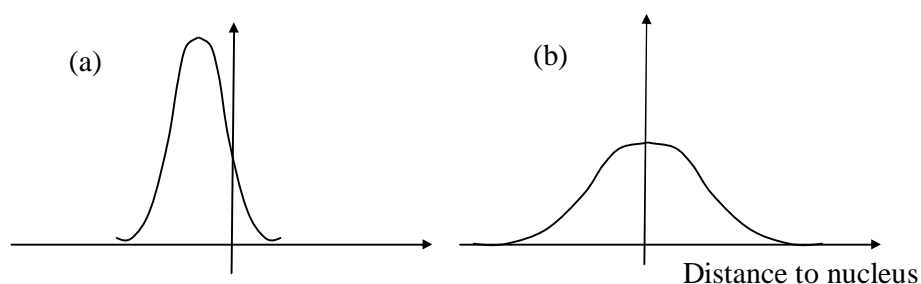


Figure 5.2: Mathematical representation of a (a) “classical” Gaussian function and (b) a diffuse Gaussian function

5.2.7. Post-Hartree-Fock methods

In computational chemistry, post-Hartree-Fock methods are the set of methods developed to improve on the HF, including the so-called electron correlation.^{1,3,4,5a} To account for electron correlation there are many post-Hartree-Fock methods, but most of them require calculations that are very time and memory consuming. The corresponding calculations are feasible for small molecular systems (less than 20 atoms).

5.2.8. Density functional theory (DFT)

Density functional theory (DFT) methods are often considered to be *ab initio* methods for determining the molecular electronic structure, even though many of the most common functionals use parameters derived from empirical data, or from more complex calculations. The DFT formalism is developed in terms of the total one-electron density rather than the wave function.^{1,3,4,5a} The resulting equations account for dynamic electron correlation. In the corresponding Hamiltonian the so-called exchange-correlation functional is approximated. The different approximations (*i.e.*, the different functionals) give the name of the different methods. DFT calculations are computationally less demanding than the post-HF methods and can be very accurate.

Some methods combine the density functional exchange functional with the Hartree-Fock exchange term and are known as Hybrid Functional Methods. These methods are a class of approximations to the exchange-correlation energy functional in density functional theory (DFT) that incorporate a portion of exact exchange from Hartree-Fock theory with exchange and correlation from other sources (*ab initio*, such as LDA, or empirical). Examples of hybrid functionals (in Gaussian 03) are B3LYP, B3P86, B1B95, B1LYP, MPW1PW91, B97, B98, B971, B972, PBE1PBE, O3LYP, BHandH, BHandHLYP, BMK, etc.

5.2.9. Programs

Many programs for molecular electronic-structure calculations exist.^{1,5a} *Gaussian* (www.gaussian.com) is the most widely used program for *ab initio* and DFT calculations. *Gaussian* exists in versions for UNIX[®] workstations and Windows[®] personal computers. It also has been a key force in the growing use of quantum

chemistry calculations by chemists, since it is an “easy-to-use” program that allows a very wide variety of quantum-mechanical methods.

5.2.9.1. Calculation of molecular properties from approximate molecular wave functions

Here, some practical information that is used to perform a quantum chemical calculation on a molecule is discussed.^{1,5a} A single-point calculation is only done at a single fixed molecular geometry specified by the user. In a geometry-optimization, the quantum-mechanical program will vary the locations of the nuclei so as to locate a minimum in the electronic energy, E_e . One calculates the molecular wave function and electronic energy for many different configurations of the nuclei, varying the bond distances, bond angles, and dihedral angles to find the minimum-energy conformation. A geometry-optimization calculation consists of many single-point calculations, with each single-point energy calculation followed by an energy-gradient (derivative of the energy versus nuclear coordinates) calculation for an initially guessed geometry to help the program decide on the next geometry to try. The geometry-optimization calculation continues until the magnitude of the gradient is very close to zero, indicating that an energy minimum has been found. Geometry-optimization calculations for large molecules are too time consuming to be done with high-level methods. Since an accurate geometry can usually be found with a low-level method, a common procedure is to do a low-level calculation to find the geometry and then use this geometry in a single-point high-level calculation of the energy.

The geometry-optimization process locates the energy minimum that is closest to the starting geometry. For example, if one does a geometry-optimization calculation of butane and inputs an initial geometry that has a CCCC dihedral angle

close to 60° , the program will converge to the geometry of the *gauche* conformer, whereas if one starts with the CCCC dihedral angle close to 180° , the program converges to the *trans* conformer. The *trans* conformer is the global minimum for butane, meaning that it has the lowest energy of all the conformers, whereas the *gauche* conformer is only a local minimum, meaning that its energy is the minimum energy for all geometries in its immediate vicinity. Every conformer lies at a local minimum of energy.

In a vibrational-frequency calculation, the program calculates the molecular vibration frequencies. A vibrational-frequency calculation must be preceded by a geometry-optimization, since vibrational frequencies calculated for a geometry that is not at an energy minimum are meaningless.

5.3. General presentation of chemical interactions

Intermolecular interactions involving aromatic rings are key processes in biological recognition but also in chemical reactions.⁶ There are several effects to be taken into account for any non-covalent interaction between two molecules^{1,2,7,8}:

- a) Van der Waals interactions, which are the sum of the dispersion and repulsion energies. These define the size and shape specificity of the interaction.
- b) Induction energy, which is the interaction between the static molecular charge distribution of one molecule and the induced charge distribution of the other.
- c) Electrostatic interactions between static molecular charges.
- d) Hydrogen bonding, which occurs between polar covalent molecules that possess a hydrogen bond and an extremely electronegative element, specifically - N, O, and F.

Due to strong and highly directional nature, hydrogen bonding has been described as the "master key" interaction in supramolecular chemistry. An excellent

example is the formation of carboxylic acid dimers, which results in the shift of the $\nu(\text{OH})$ infrared stretching frequency from about 3400 cm^{-1} to about 2500 cm^{-1} . Typically, hydrogen bonded H...O distances are 2.50-2.80 Å in length although in some cases are around 1.8 Å. Hydrogen bonds are accountable for the overall shape of proteins, recognition of substrates by various enzymes, and for the double helix structure of DNA. Hydrogen bonds also can be found in a range of lengths, strengths and geometries.

Over the past years long range interaction involving π electron regions have been demonstrated to influence supra-molecular architectures. These interactions can be surprisingly strong, or at times, extremely weak depending on the matter of context. Three general π binding forces are discussed here:

- the cation- π interaction,
- the polar- π interaction, and
- the aromatic-aromatic interaction (or π - π interaction)

5.3.1. Cation- π interactions

Cation- π interaction is a non-covalent electrostatic binding force between a cation and the face of a simple π system such as benzene or ethylene.^{1,2} This quite strong interaction has begun to be recognized only in recent years and is making considerable contributions to molecular recognition phenomena in both biological and synthetic systems. Figure 5.3 shows that in the gas phase the cation- π interaction can be quite strong whereby the Li^+ ---benzene interaction can be even comparable to the strongest hydrogen bond.

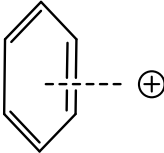
	M^+	$-^a G^\circ$ (kcal/mol)
	Li^+	38
	Na^+	27
	K^+	19
	Rb^+	16

Figure 5.3: Binding energies for simple cations to benzene in gas phase.^{1,2}

5.3.2. Polar- π interactions

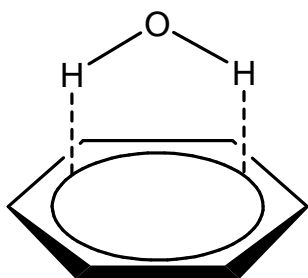


Figure 5.4: π Hydrogen bonds.^{1,2}

Water can bind cations electrostatically by aligning its large permanent dipole moment appropriately. Benzene too aligns its large permanent quadrupole moment appropriately to bind cations electrostatically. In fact, a polar molecule has a substantial, permanent dipole

moment. But why should not a quadrupole moment to be considered just as a dipole? If a molecule can bind ions strongly through a predominantly electrostatic interaction, it should be considered to be polar. Benzene is polar, it is just quadrupolar rather than dipolar.^{1,2}

Water binds water well, and benzene binds water, too. The binding energy between benzene and water is 1.9 kcal/mol in gas phase, and the geometry is as anticipated with the water hydrogen atoms (the positive end of the water dipole) pointed into the benzene ring (Figure 5.4). Likewise, ammonia binds to benzene with 1.4 kcal/mol of binding energy in gas phase.^{1,2} Such interactions have been termed as hydrogen bonds to benzene. On the other hand, this seems to be pushing the hydrogen bond description a bit far. A preferable term is a polar- π interaction, which will be an

indication of a conventionally polar molecule interacting with a quadrupole moment of a π system. Any hydrogen bond donor, such as an amide NH or an alcohol OH, will experience a favorable electrostatic interaction with the face of a benzene ring. This is because of the large bond dipole associated with the hydrogen bond donor. Even though they are weaker than cation- π interactions, polar- π interactions are also found in protein structures, and are vital contributors to solid state packing interactions.

5.3.3. Aromatic stacking interactions

In organic chemistry, aromatic stacking interaction is a phenomenon affecting aromatic compounds and functional groups.¹⁰ Due to strong van der Waals forces between the surfaces of flat aromatic rings, these groups in different molecules tend to align themselves like a stack of coins. This nature of interaction influences the properties of polymers as diverse as polystyrene, DNA and RNA, proteins and peptides.

In 1990, Hunter and Sanders proposed a model for aromatic interactions.⁹ Molecular mechanics calculations on linked cofacial porphyrin dimers consistently predicted a perfectly stacked arrangement of the porphyrin rings, whereas experimental studies show an offset arrangement.

A simple electrostatic model of a π -system was proposed. This includes an aromatic ring with a positively charged σ framework sandwiched between two regions of negatively charged π -electron density/clouds (Figure 5.5).⁸

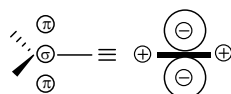


Figure 5.5: An sp^2 hybridized atom in a π -system.^{8,9}

A set of point charges was used to represent the electrostatic charge distribution of the molecule (Figure 5.7). This was used to calculate the electrostatic interaction between two such π -systems resulting in the sum of the charge-charge interactions. In the simplest case, a charge of +1 at the nucleus of the atom was used for each carbon atom in the π -system. This was followed by taking into account two charges of $-1/2$ at a distance of δ , above and below the plane of the π -system.

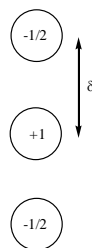


Figure 5.6: Model for an atom which contributes one electron to the molecular π -system; projection parallel to the plane of the π -system.^{8,9}

According to Hunter and Sanders, σ interactions are not due to an attractive electronic interaction between the two π -systems.⁹ They take place when the attractive interactions between π -electrons and the σ scaffold outweigh unfavorable contributions such as π -electron repulsion.

5.3.3.1. A set of rules on π - π interactions

Geometrical requirements.

To draw some general conclusions about the preferred geometries of π - π interactions, Hunter uses the set of three charges as shown in Figure 5.7. These correspond to an idealized π -system or π -atom that involves the interaction between two such π -atoms (for a fixed vertical separation of 3.4 Å). Figure 5.8 shows how the

electrostatic π - π interaction varies as a function of their relative orientation in the absence of any polarization effects.

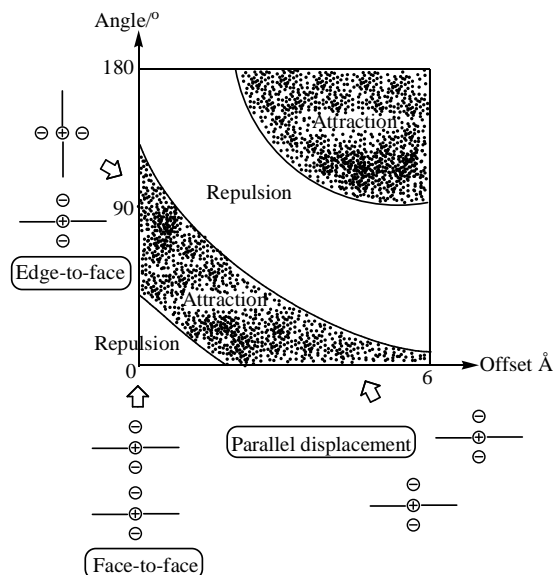


Figure 5.7: Interaction between two idealized π -atoms as a function of orientation: two attractive geometries and the repulsive face-to-face geometry are illustrated. (y-axis: angle of anti-clockwise rotation about the central positive charge of the upper π -atom; x-axis: offset toward the right-hand side of the diagram).^{8,9}

The following terms will be used to describe the geometry of interaction:

- Edge-to-face ($\text{C-H}\cdots\pi$): describes the favorable T-shaped, perpendicular arrangement of aromatic rings where the σ - attraction dominates.
- Stacked (face-to-face/sandwich): describes the non favorable parallel arrangement due to domination of π - electronic repulsion resulted in the repulsive zone.
- Offset stacked (parallel displacement) describes the favorable parallel arrangement where electrostatic interaction σ - attraction is the dominant interaction.

From the analysis of the results summarized in the diagram (Figure 5.7), three rules can be enunciated for non polarized π -system:

Rule 1: - repulsion dominates in a face-to-face π -stacked geometry.

Rule 2: $-\sigma$ attraction dominates in an edge-on or T-shaped geometry.

Rule 3: $-\sigma$ attraction dominates in an offset $-\pi$ -stacked geometry (Figure 5.8).

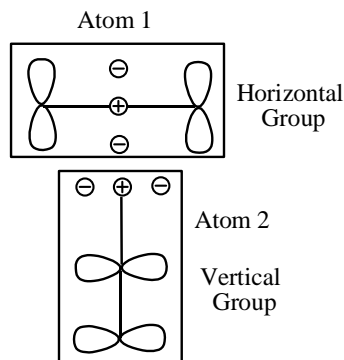


Figure 5.8: Edge-on or T-shaped geometry.⁹

Experimental data for the validity of these rules comes from the crystal structures of simple aromatic compounds. In general, two types of geometry are observed:

- edge-to-face relationships, which give rise to the characteristic herring bone pattern;
- offset stacked relationships.

5.3.3.2. Effects of polarization between π -systems polarized by heteroatoms

The face-to-face stacked geometry is constantly favored by van der Waals interactions and solvophobic effects. Commonly, $-\pi$ repulsion disfavors face-to-face stacked geometry. In spite of this, the presence of strongly-polarizing atoms has a major effect on the electrostatic interaction. The sum of electrostatic interaction is plotted for a range of π -electron densities on atom 1 (Figure 5.9) interacting with an atom 2 which is neutral (non-polarized), electron-rich or electron-deficient.

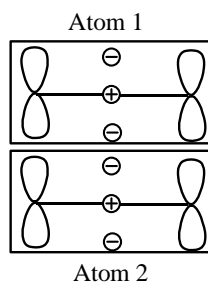


Figure 5.9: Face-to-face π -stacked geometry.⁹

This has lead Hunter and Sander to three additional rules:

Rule 4: For interactions between highly charged atoms, charge-charge interactions dominate.

Rule 5: A favorable interaction with a neutral or weakly polarized site requires the following π -polarization:

- a) a π -deficient atom in a face-to-face geometry;
- b) a π -deficient atom in the vertical T-group in the edge-on geometry;
- c) a π -rich atom in the horizontal T-group in the edge-on geometry.

Rule 6: A favorable interaction with a neutral or weakly polarized site requires the following σ polarization:

- a) a positively charged atom in a face-to-face geometry;
- b) a positively charged atom in the vertical T-group in the edge-on geometry;
- c) a negatively charged atom in the horizontal T-group in the edge-on geometry.

Inverting the polarizations in rules 5 and 6 leads to repulsion.

Table 5.0: Electrostatic contribution to π -stacking interactions between polarized π -systems (in kJ/mol).⁹

$-R_1^b$	$-R_2^b$	Orientation ^a					
		1	2	3	4	5	6
-H	-H	14.9	14.8	-2.0	-2.0	-1.9	-2.0
-H	-NH ₂	17.8	17.6	-1.4	-1.1	-1.0	-1.4
-H	=O	-1.5	-1.7	-5.3	9.1	9.1	-5.3
=O	=O	22.7	-13.6	-0.3	-1.4	0.6	-1.4
=O	-NH ₂	3.3	-1.7	-7.6	-7.5	10.9	11.6
-NH ₂	-NH ₂	25.9	22.2	-0.3	-0.4	-0.6	-0.4

^aSee Figure 5.10 for an illustration of orientations of 1-6. Negative values indicate attractive interactions, while positive values correspond to repulsive interactions. ^b6H corresponds to benzene; -NH₂ is *p*-phenylenediamine; =O is *p*-benzoquinone.

Table 5.0 demonstrates the crucial importance of the geometry of interactions in polarization effects, which then influences π - π interactions. Interactions between three different π -systems were considered:

- benzene, a non polarized π -system
- *p*-phenylenediamine, an electron donor and
- *p*-benzoquinone, an electron acceptor.

The polarization of an electron donor results in a net negative charge of aromatic ring and the substituents possess a net positive charge. In contrast, the polarization of an electron acceptor results in a net positive charge of the aromatic ring and the substituents possess a net negative charge.

The predicted magnitudes of the electrostatic components of the π - π interaction energies for all likely combinations of these π -systems are shown in Table 5.0. Figure 5.10 illustrates all the six orientations of the π -systems. It is noteworthy that the magnitudes and conclusions should be considered as qualitative only. The area of π -overlap is proportional to the contribution of van der Waals interactions to the total energy and will vary with solvent as outlined above.

All the values in Table 5.3 can be interpreted by using a set of rules. In general, offset stacking (orientations 3-6) is attractive, and face-to-face stacking (orientations 1 and 2) is repulsive. However, rule 4 predicts that when the atoms at the site of contact are π -deficient, π -overlap is favorable and, therefore, attractive face-to-face stacking is predicted for the acceptor-acceptor interaction in orientation 2 (Figure 5.10). When the atoms at the site of contact are π -rich, large repulsive interactions are predicted.

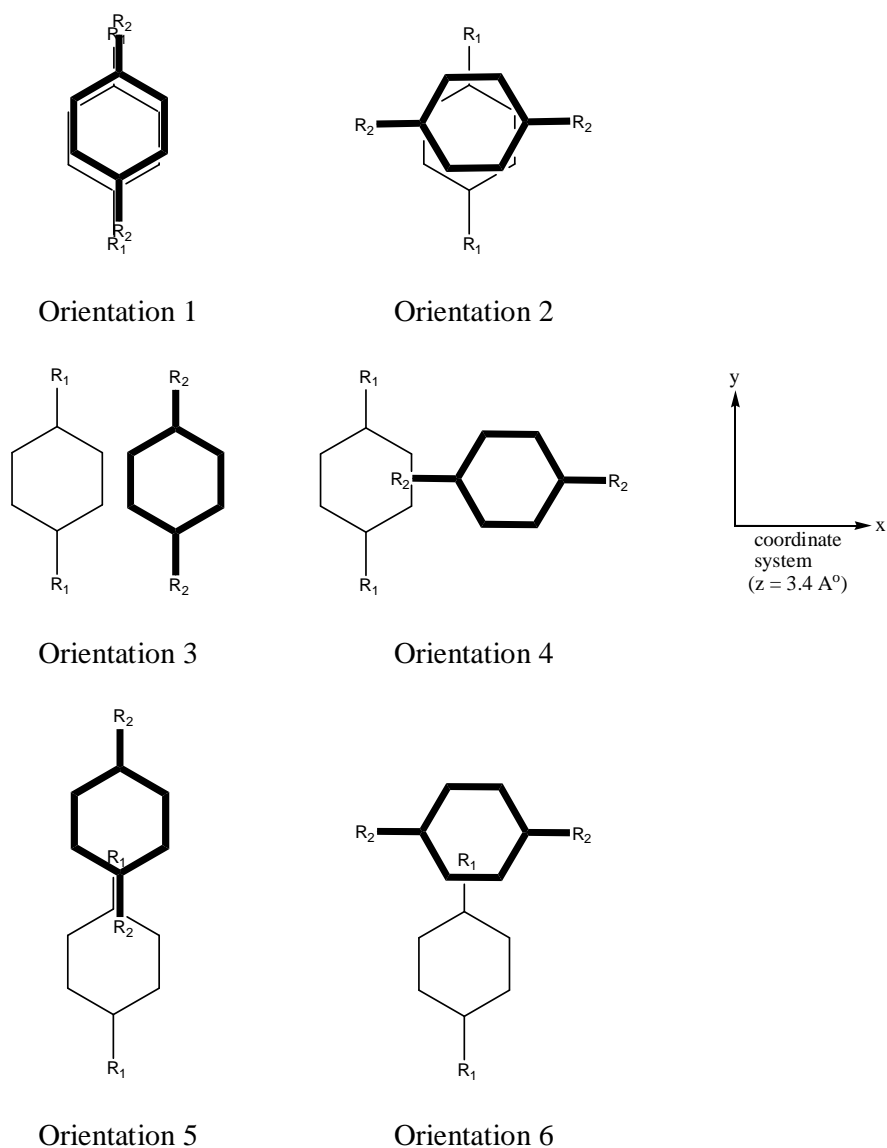


Figure 5.10: Orientations for the π - π interactions between polarized π -systems. R_1 and R_2 are the polarizing groups.⁹

Burguete *et al.* (2002)¹¹ reported the crystal structure of tetrabenzylated macrocycles revealing several intermolecular aromatic edge-to-face interactions that are important in the three-dimensional growing of the crystalline structure. Figure 5.11 presents the three different aromatic-aromatic edge-to-face interactions.

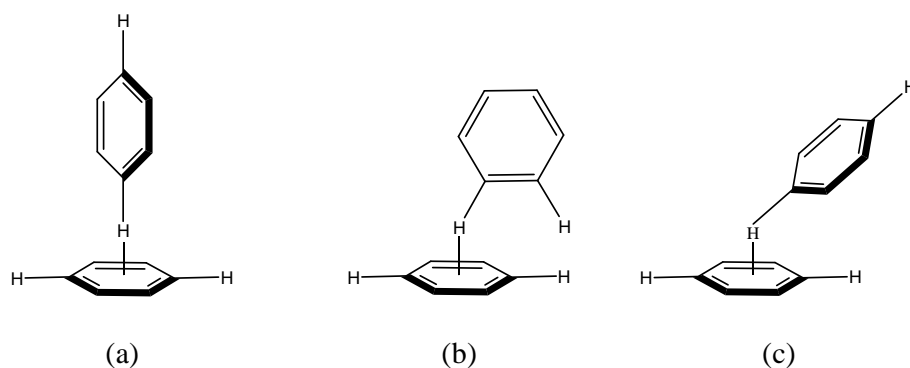


Figure 5.11: Limit structures possible for edge-to-face aromatic interactions: a) T-shaped, b) edge-tilted-T, and c) face-tilted-T.¹¹

The substituent in the phenyl ring interacting in the edge manner can also be known as the one acting as hydrogen donor. The main structural parameters for inter-ring interactions are defined in Figure 5.12. Aromatic edge-to-face interactions play a vital role in the self-organization that results in crystal formation and in determining the nature of the observed crystal packing.

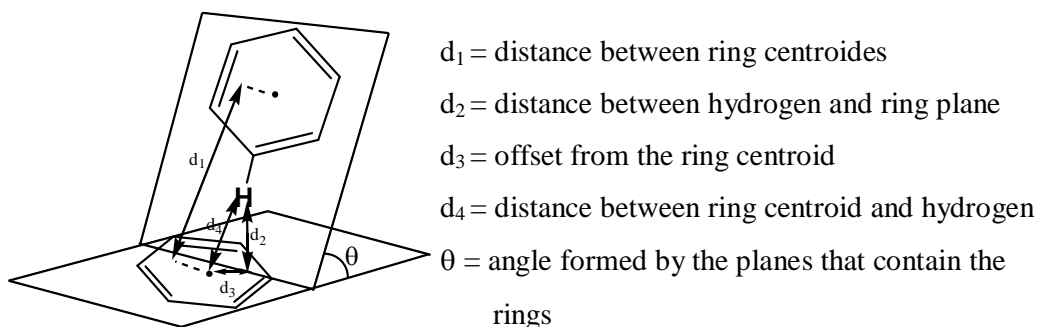


Figure 5.12: Schematic representation of the angle θ and distances d_1 - d_4 used for describing edge-to-face interactions.¹¹

For instance, in the work of Burley and Petsko (1985)¹² mentioned previously, that in proteins there is a preference for edge-to-face type interactions between phenyl rings. The predominance structures present a distance between phenyl ring centroids of 4.5 to 7 Å and a dihedral angle of 60 to 90°.

Coates *et al.* used stacking interactions in solid state to control the photodimerization of olefins.¹³ In a similar way on how the benzene and hexafluorobenzene produce face-to-face stacks, (E)-pentafluorostilbene crystallizes with long stacks of alternating phenyl and pentafluorophenyl rings. These stacks then lead to a single isomer of the cyclobutane photodimer.⁸

In summary, it is a π - σ attraction rather than a π - π electronic interaction that leads to favorable interactions. Hence, the geometry of an interaction can be determined by electrostatic effects, while van der Waals interactions (and solvophobic effects) make the major contribution to the magnitude of the observed interaction. Sanders and Hunter⁹ emphasize the importance of the interactions between individual pairs of atoms rather than molecule as a whole. Although, their approach has been somewhat successful, there is still an enormous deal of debate over the characteristics of π - π stacking interactions. The key energetic contributions to these interactions are van der Waals dispersion and electrostatics but there is still extensive debate about the dominant force.²

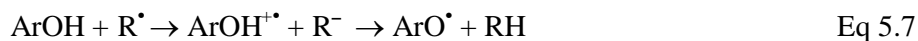
5.4. Methods and results: modeling of stilbenoids and their oxidized forms

To understand stilbene dimerization/oxidative coupling, the redox properties of the stilbenes need to be understood. The redox reactivity of phenolic compounds (ArOH) can be explained by three different chemical pathways¹⁴:

- (i) H atom transfer (HAT) mechanism:



- (ii) electron transfer (ET) mechanism:



(iii) sequential proton loss electron transfer (SPLET) mechanism:



The first mechanism is governed by the O-H bond dissociation enthalpy (BDE). In this mechanism, the H atom is directly transferred from the molecule to the radical/oxidant. The second mechanism is governed by the ionization potential and the reactivity of the $\text{ArOH}^{+\bullet}$ cation. In this case the electron is transferred from the molecule to the radical/oxidant, leading towards indirect H^+ abstraction. In the third mechanism, the polyphenol is first deprotonated and the electron transfer to the free radical can occur from the ArO^- anion. This mechanism is not possible in acidic solution, is favored in alkaline condition and depends on polyphenol OH group acidity under neutral conditions. Anyhow, each mechanism yields a ArO^\bullet mechanism, which must be relatively stable so that the reactions are thermodynamically favorable. Therefore, bond dissociation enthalpy (BDE) and ionization potential (IP) calculations were performed for partially protected and fully protected stilbenes for comparison purpose. So as to reinforce the above understandings, spin density, conformation analysis, molecular orbitals of the above mentioned stilbenes were also investigated. All the calculations were performed in University of Limoges, France, under the supervision of Dr. Patrick Trouillas. All these calculations were carried out in Gaussian03.^{5b}

5.4.1. Definition and calculation method of the bond dissociation energy

The bond dissociation enthalpy (BDE) is a measure of the bond strength of a chemical bond. It is defined as the standard enthalpy change when a bond is cleaved by homolysis, with reactants and products of the homolysis reaction. It is usually

given at 298 K. Bond dissociation is an endothermic process, where the lower the BDE, the easier the bond cleavage.

Eq 5.6 corresponds to the homolytic dissociation of an O-H bond. This reaction can occur on each OH group of the phenolic compound/stilbenoids, depending on the BDE of the OH group and on the enthalpy difference ΔH_1 of eq 5.6. Eq 5.9 gives the BDE of the reaction at a given temperature.

$$\text{BDE} = H(\text{ArO}^\bullet) + H(\text{H}^\bullet) - H(\text{ArOH}) \quad \text{Eq 5.9}$$

The BDE is an intrinsic thermodynamical parameter of a given OH group in a phenolic compound/stilbenoid whereas ΔH_1 depends on the radical/oxidant reacting with the phenolic compounds/stilbenoids. In order for the oxidant/radical R^\bullet to react with the stilbene, the OH group must possess a BDE low enough so that ΔH_1 is negative and reaction 5.6 is exothermic.

5.4.1.1. Bond dissociation energy calculation method

Several approaches can be used to calculate redox properties of phenolic compounds. DFT seems to be the most reliable approach to obtain reliable polyphenolic BDE values that are close to experimental data.^{15,16} Within the DFT formalism, the functional and the basis set significantly influence the accuracy of the results. The combination of the B3P86 functional with a relatively large basis set [6-311 + G(d,p)] leads to excellent results for the BDE estimation of phenol in the gas phase compared to the experimental data ($\text{BDE}_{\text{theoretical}} = 86.9 \text{ kcal/mol}$ versus $\text{BDE}_{\text{experimental}} = 87.0 \pm 1.5 \text{ kcal/mol}$).¹⁷ Compared to the widely used B3LYP functional, B3P86 calculations show an improvement in the BDE values by about 4 kcal/mol for phenol and catechol. Therefore, here the DFT/B3P86 approach with basis set 6-31+G(d,p) and/or 6-31G(d) was used for stilbenoids in gas phase. Geometry

optimization of each stilbene radical was performed starting from the optimized structure of the parent stilbene unit after the removal of H atom at position 12 or 3. This was followed by frequency calculations to (i) confirm the absence of any negative frequency so that convergence to local minima on the energy surface is reached, and (ii) to allow the temperature correction allowing to calculate enthalpies at 298K. All calculations were carried out with the Gaussian03 software from Gauss Inc, USA.

5.4.2. Definition and calculation method of the ionization potential

The ionization potential, ionization energy or E_I of an atom or molecule is the energy required to remove one electron from one isolated gaseous atom or ion. The greater the ionization energy, the more difficult it is to remove an electron. The ionization potential is an indicator of the reactivity of a chemical species. The second pathway is governed by the electron transfer capacity to the radical R^\bullet (ΔH_2 in eq. 5.10) and by the ionization potential (IP in eq 5.11):

$$\Delta H_2 = [H(\text{ArOH}^{+\bullet}) + H(R^\bullet)] - [H(\text{ArOH}) + H(R^\bullet)] \quad \text{Eq 5.10}$$

$$IP = E(\text{ArOH}^{+\bullet}) - E(\text{ArOH}) \quad \text{Eq 5.11}$$

The second step of this reaction is the heterolytic O-H bond dissociation, which is strongly exothermic for phenolic compounds.

5.4.2.1. Ionization energy calculation method

The ionization energy calculation was performed using DFT/B3P86 approach with basis set 6-31+G(d,p) and/or 6-31G(d) to stilbenoids in gas phase. Geometry optimization of each stilbene radical cation was performed starting from the optimized structure of the parent stilbene unit. This was followed by frequency

calculations to confirm convergence to local minima on the energy surface. All calculations were carried out with the Gaussian03 software mentioned above.

5.4.3. Results and discussion

In attempts to understand the redox properties of stilbenoids in oxidative couplings/stilbene dimerization the following parameters were quantum-chemically measured:

- a) O-H bond dissociation enthalpy (BDE) to understand the HAT mechanism for:
 - i) OH groups substituted at positions 3 and 12 of resveratrol **1.0**
 - ii) OH groups substituted at position 12 of pterostilbene **1.2** and demethoxypterostilbene **2.56** respectively.
- b) The ionization potential (IP) to explain the ET mechanism and $\text{ArOH}^{+\bullet}$ stability for
 - i) 12-acetoxy-3,5-dimethoxystilbene **2.46**
 - ii) 12-acetoxy-3,4-dimethoxystilbene **5.0**
 - iii) 12-benzyloxy-3,4-dimethoxystilbene **4.40**
 - iv) Pterostilbene **1.2**
 - v) Demethoxypterostilbene **2.56**

The optimized geometries of the above listed stilbenes are shown in Figure 5.13.

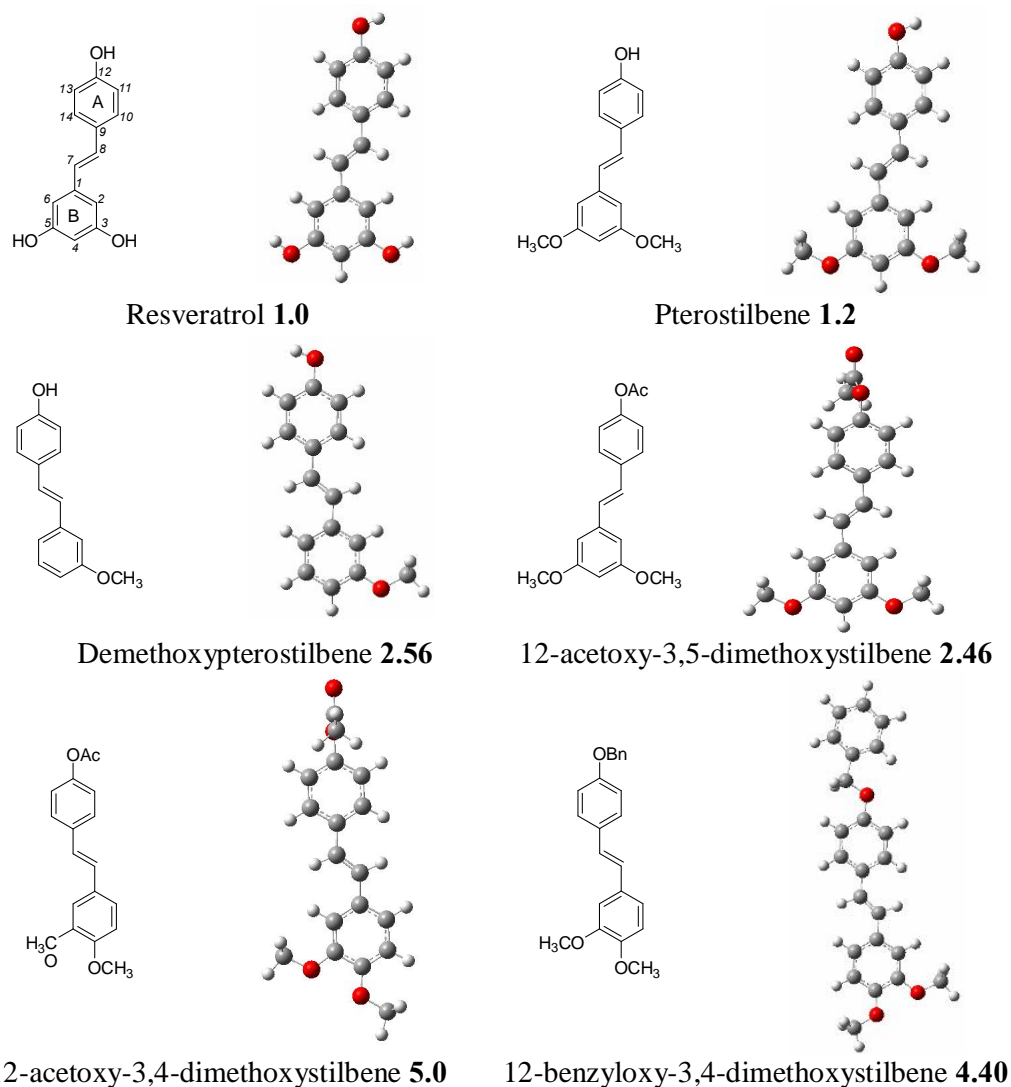
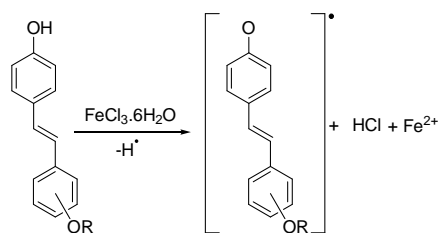


Figure 5.13: Optimized geometries of stilbene derivatives after calculations.

5.4.3.1. H atom transfer (HAT) mechanism and BDE calculations



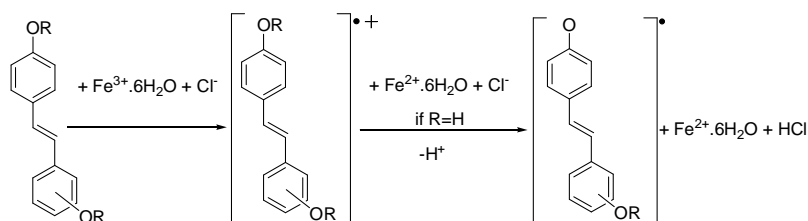
Scheme 5.1: H atom transfer mechanism of stilbenoid.

The BDE for OH groups of the three stilbenoids were calculated as shown in Eq 5.9 and tabulated in Table 5.1. The bond dissociation enthalpy (BDE) for the *para* substituted 12-OH groups of resveratrol **1.0**, pterostilbene **1.2** and demethoxypterostilbene **2.56** share similar values (~81 kcal/mol). In contrast BDE for OH group at position 3 of resveratrol has the highest value of 88.25 kcal/mol. These results were consistent with those of Huai Cao *et al.*¹⁸ who reported that the BDEs of substituted OH groups at positions 3 and 12 of resveratrol calculated at B3LYP/6-311G** level are 89.9 kcal/mol and 84.5 kcal/mol, respectively. This indicates that H atom at *para* (12-OH) position is easier to be abstracted due to lower BDE. The O-H BDE of stilbene is mainly governed by the stability of its phenoxyl radical generated after H-abstraction from the native stilbene. The spin delocalization of the unpaired electron determines the stability of stilbene radical (refer section on spin density).

Table 5.1: Calculated BDE for some of the stilbenoids.

	BDE, $\hat{e}H$ (kcal/mol) 6-31+G(d,p)
3-OH substituted 1.0	88.25
12-OH substituted 1.0	81.20
12-OH substituted 1.2	81.23
12-OH substituted 2.56	81.36

5.4.3.2. Electron transfer mechanism and IP calculations



Scheme 5.2: Electron transfer mechanism for stilbenoid.

To estimate the contribution of the electron transfer (ET) mechanism and the $\text{ArOH}^{\bullet+}$ stability, the ionization energy of the 5 stilbenoids (partially and fully protected) were calculated as shown in Eq 5.11 and tabulated in Table 5.2. From these calculations, stilbenes with resorcinolic substitution pattern **1.2**, **2.56** and **2.46** were found to have similar ionization energies (168.95, 170.21 and 168.13 kcal/mol respectively). In contrast, stilbenes with catechol substitution pattern were shown to have lower ionization energy with a difference of 9 kcal/mol for **5.0** and 12 kcal/mol for **4.40** with respect to the average IP value obtained for resorcinolic substituted stilbenes **1.2**, **2.56** and **2.46**. These differences can be rationalized by the enhancement of the stabilization of the π electrons in the stilbene radical cation due to the presence of substituent group at the *para* position. Globally speaking for these compounds the ET process forms an intermediate radical cation highly unstable. This indicates that the mechanism is a thermodynamically unfavorable for occurrence of those compounds, as compared to the sheer O-H bond cleavage.

Table 5.2: IP values of stilbenoids

	IP(kcal/mol) 6-31+G(d,p)	IP(kcal/mol) 6-31G(d)
Pterostilbene 1.2	168.95	164.48
Demethoxypterostilbene 2.56	170.21	165.92
12-acetoxy-3,5-dimethoxystilbene 2.46	168.13	-
12-acetoxy-3,4-dimethoxystilbene 5.0	160.25	-
12-benzyloxy-3,4-dimethoxystilbene 4.40	157.53	-

5.4.3.3. Conformational studies

A conformational analysis has been performed for stilbenes with respect to the two torsion angles $\theta = \text{C6-C1-C7-C8}$ and $\phi = \text{C7-C8-C9-C14}$ (Table 5.3, Figure 5.13). Compounds **2.56** and **5.0** are planar structures. Stilbenes with resorcinolic

substitutions pattern **1.0** ($\approx 7^\circ / \approx 11^\circ$), **1.2** ($\approx 6^\circ / \approx 9^\circ$) and **2.46** ($\approx 8^\circ / \approx 8^\circ$) exhibit a slight distortion compared to planarity. Stilbene radicals derived from 12-OH of **1.0**, **1.2**, **2.56** and radical cations derived from **1.2**, **2.56**, **2.46**, **5.0** and **4.40** gain planarity after removal of H atoms and electrons, respectively. This appears as a consequence of an effective electron delocalization over the entire structure. However, stilbene radical derived from 3-OH of **1.0** (Figure 5.14) lost its planarity as the electron conjugation is destroyed. This translates in the highest occupied molecular orbital (HOMO), being localized only over the B ring.

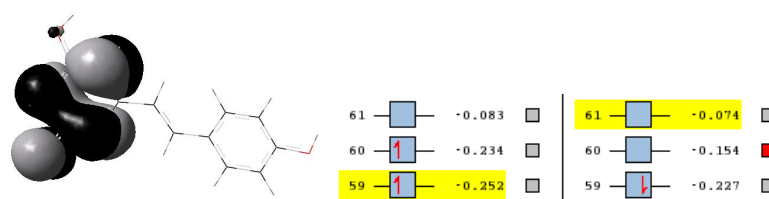


Figure 5.14: SOMO (singlet Occupied Molecular Orbital) of resveratrol radical.

Table 5.3: Torsion angles values for stilbenoids.

	Torsion angle	
12-benzyloxy-3,4-dimethoxystilbene 4.40	1.4°	1.6°
12-acetoxy-3,4-dimethoxystilbene 5.0	1.9°	0.6°
Resveratrol 1.0	7.0°	11.0°
Pterostilbene 1.2	6.0°	9.0°
12-acetoxy-3,5-dimethoxystilbene 2.46	8.0°	8.0°

5.4.3.4. Spin density

The spin density is calculated as the total electron density of up spin electrons minus the total electron density of down spin electrons. It gives the distribution of a radical unpaired electron, which, in turn, decides on the stability of the radicals. It was computed at B3P86/6-31 G(d) level. In general the more delocalized the spin density

in the radical, the easier the radical is formed and the lower the BDE. Figure 5.15 shows the calculated spin density of the radicals obtained after H abstractions from the OH groups of stilbenes.

Calculation shows that, when the H atom is abstracted from the 12-OH group of resveratrol **1.0**, the spin density of the radical **5.1** is distributed throughout the O-12, A ring and C-7 of the olefinic bond (Figure 5.15). This results in stabilizing the radical *via* a semi-quinone resonance structure. The observed result is in accordance with the reported data by H. Cao *et al.* (2003).¹⁸

We can apply the same explanation to the other partially substituted stilbene radical species such as **5.3** and **5.5** (Figure 5.15), which derived from **1.2** and **2.56** respectively. However, H atom transfer from 3-OH of resveratrol indicates that the spin density is localized at the O-3 and the ring B only (**5.2**), Figure 5.15. This is due to the non planarity of the stilbene radical whereby the delocalization of the electrons are unable to be extended to the C-7 of the olefinic bond. This means that the radical is not easy to be formed and explains why the BDE is higher than that of the 12-OH stilbene.

Clearly, when a stilbene undergoes an electron transfer mechanism, a stilbene radical cation is produced. When an electron is removed from the ground state of **1.2**, the resulting stilbene radical cation **5.4** shows a high spin density of 0.36 at C-4. This is true for **5.8** where the spin density at C-4 is of the same order of magnitude (0.42). This indicates a weak delocalization of electrons, which then results in the formation of an unstable radical and a high IP. Compound **5.6** shows a slight better delocalization with spin densities of 0.28, 0.24 and 0.19 at C-4, C-6 and C-7 respectively. Catechol substituted stilbene, **5.7** shows a higher spin density of 0.2 at C-8 than C-7, which is only 0.05. In contrast, **5.9** shows a near equal distribution of spin density of 0.12 and 0.13 at C-8 and C-7 respectively.

The above observed trend suggests that 12-OH stilbenes are more likely to undergo H atom transfer mechanism than an electron transfer mechanism. This can be rationalized through the stable formation of semi-quinone radical resonance structures.

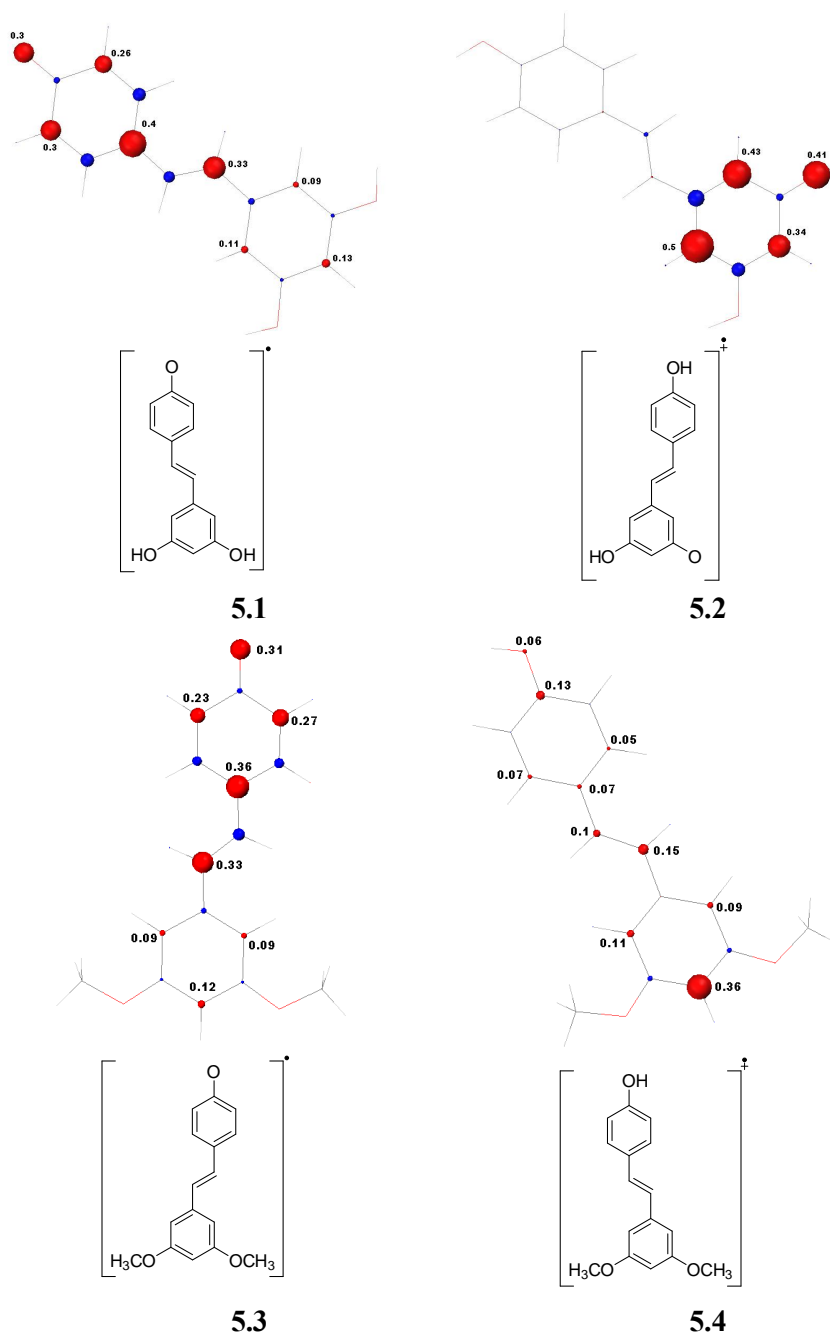
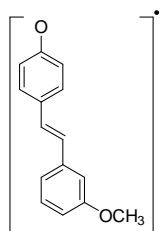
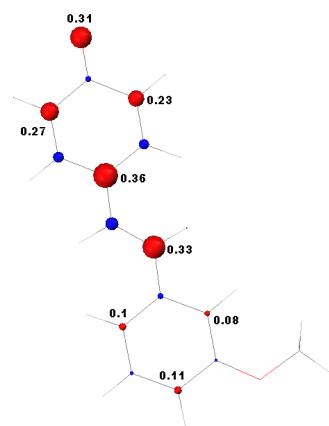
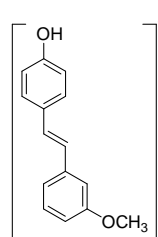
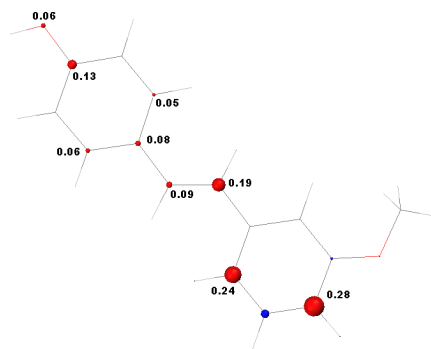


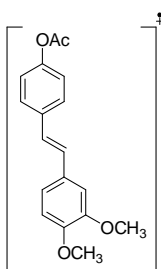
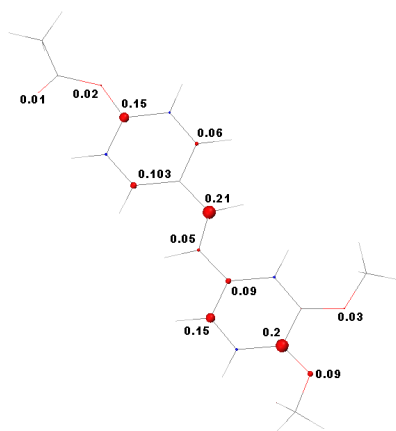
Figure 5.15: Spin densities of stilbenoid radicals and radical cations.



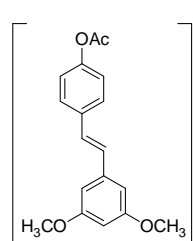
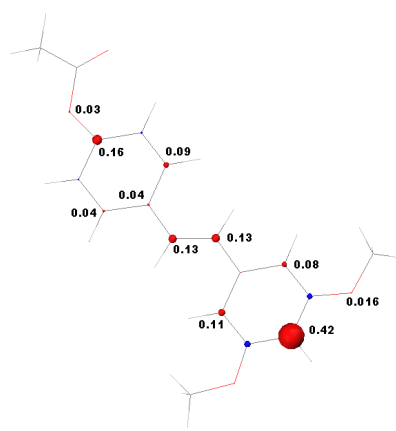
5.5



5.6



5.7



5.8

Figure 5.15 (cont'd): Spin densities of stilbenoid radicals and radical cations.

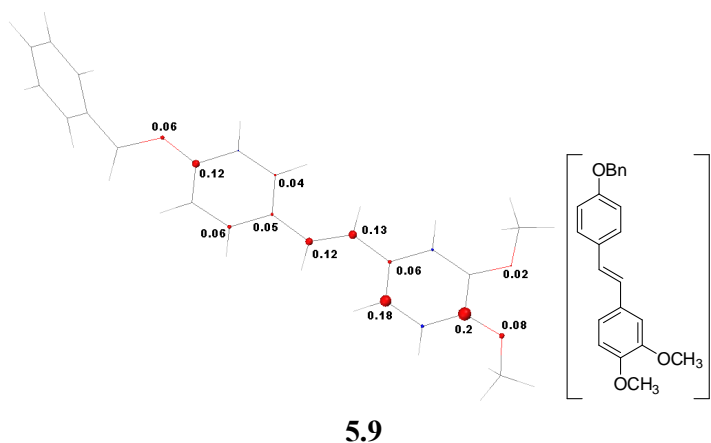
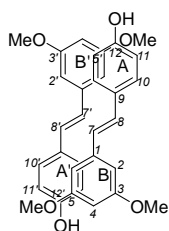


Figure 5.15 (cont'd): Spin densities of stilbenoid radicals and radical cations.

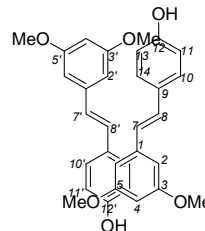
5.5. Methods and results: Modeling of stilbenes pairs

Various *Re/Re* and *Re/Si* approaches were studied for pterostilbene and demethoxypterostilbene. In addition, contribution of hydrogen bonding in pterostilbene alignment was also calculated. Alignments of oxidized stilbene species consist of stilbene radical-stilbene pairs and stilbene radical-stilbene radical pairs were also studied. The following conventions were used in the text to avoid confusion:

- Orientation: initial positioning
- Alignment: calculated for a given pair of substituted stilbenes
- Geometry: group of similar alignments
- The IUPAC numbering system is used for stilbenes as shown below.



Re/Si alignment



Re/Re or *Si/Si* alignment

All the calculations were performed in gas phase using BHandH method with 6-31G(d) as basis set.¹⁹

5.5.1. Contribution of hydrogen bonding and π - π interactions in *para* hydroxy-substituted stilbenes alignment

To measure the contribution of intermolecular interactions between two stilbene units, calculations were performed at the BHandH/6-31G(d) level. For comparison purpose, the modeling of pairs of stilbenes with and without hydroxy groups was performed. We have only considered a *Re/Si* approach and head-to-tail orientation for the above calculations.

The stabilizing energies of the π complex (*i.e.*, stilbene alignments) were obtained by deducting twice the electronic energy of the stilbene monomer to the electronic energy of the stilbene π complex.

In the absence of hydroxyl groups (alignment **A**, Figure 5.16), the stabilizing energy was -14.33 kcal/mol. As soon as the hydroxyl groups were introduced in the stilbene stack/alignment (**B**), the stabilizing energy became -19.29 kcal/mol. As can be seen in Figure 5.14, **A** shows parallel alignment between the two stilbene units, whereas **B** is slightly bent. This can be understood by the fact that, there is only π - π interactions involved in **A**, whereas in **B** the intermolecular interactions are governed by both π - π interactions and hydrogen bonding due to the presence of free hydroxyl groups. The H bonding contribution is around 5.0 kcal/mol. This is attributed to the presence of two equivalent H bonds (distance between OCH₃ and OH measured at 1.96 Å). In general hydrogen bonds vary in strength from very weak (0.2-0.5 kcal/mol) to extremely strong (> 37 kcal/mol). In our case the strength per H bond is about 2.5 kcal/mol, which corresponds to a relatively weak bond.²

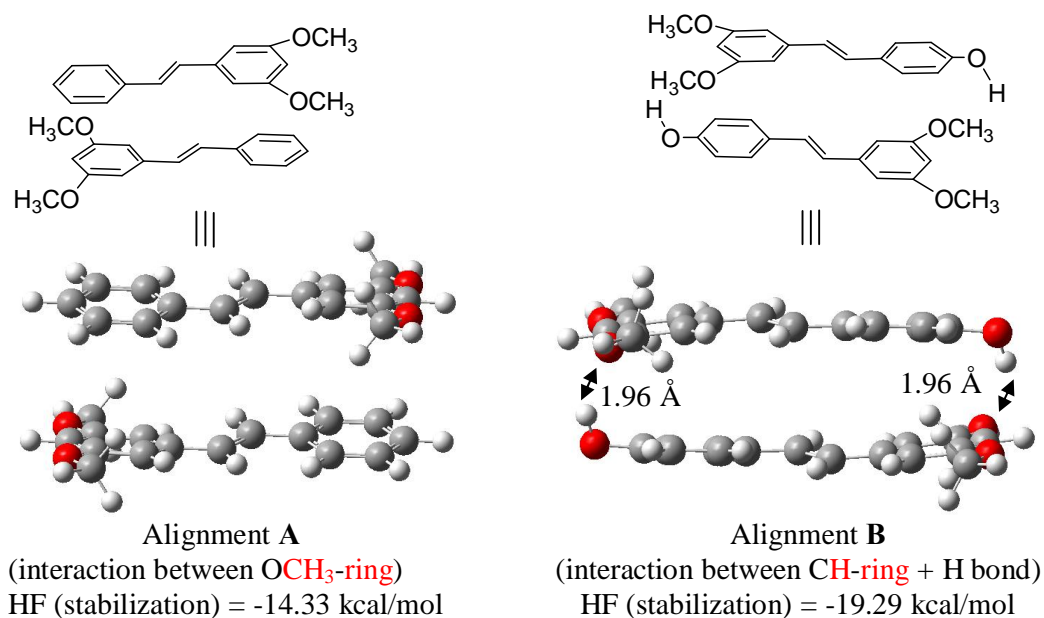


Figure 5.16: Influence of the hydroxyls on the stacking of a stilbene pair

5.5.2. Comparison of stability between head-to-head and head-to-tail alignments of stilbenes

Starting from two different geometries (head-to-tail and head-to-head) of the 12-hydroxy substituted stilbenes, alignments **B** and **C** (Figure 5.17) were obtained at the BHandH/6-31G(d) level.

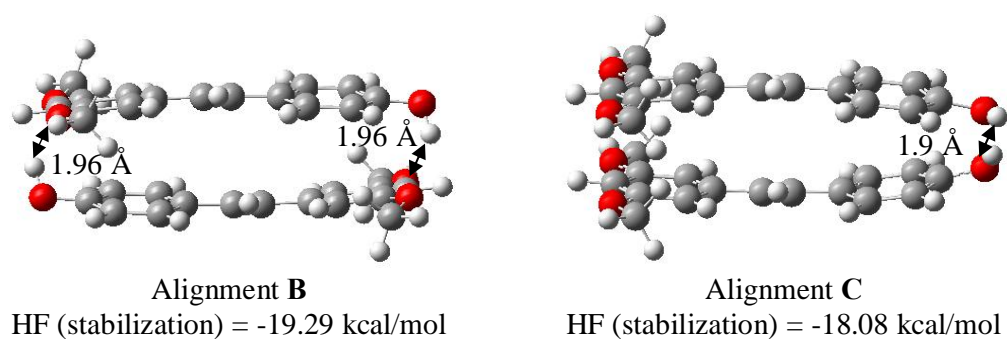


Figure 5.17: Influence of geometry type on stilbene alignment

The above models (Figure 5.17) show that the head-to-tail alignment is more stable by 1.21 kcal/mol compared to head-to-head alignment. This means that both

types of complexes exhibit a very similar stability, since 1 kcal/mol is very close to the limit of chemical accuracy.

5.5.3. Calculation results on various *Re/Si* approaches of pterostilbene units

Two pterostilbene monomers **5.2** were aligned in a *Re/Si* manner at an inter-plane distance of 3.5 Å with the five different starting geometries listed below:

- i) face to face geometry: Orientation 1
- ii) Parallel displaced geometry with an offset of 1.4 Å where a C atom of ring Bø of a given unit is placed in the center of the ring A of the opposite unit as follows:
 - a) C-6ø Orientation 2
 - b) C-2ø Orientation 3
 - c) C-3ø Orientation 4
 - d) C-5ø Orientation 5

From the results obtained, we can categorize the optimized alignments into three different geometries A, B and C.

- i) Orientation 1 produced geometry A
- ii) Orientations 2 and 5 produced geometry B
- iii) Orientations 3 and 4 produced geometry C

Geometry A

Geometry A is a parallel displaced alignment with an offset of 1.7 Å along the y axis and a distance of 3.25 Å between the two parallel planes. C-9 and C-9ø are placed explicitly above the centre of rings Bø and B respectively, while C-4 and C-4ø

are located above the centre of ring A and A respectively (Table 5.4). Hydrogen bonding does not seem to have any influence in this arrangement.

Geometry B

Geometry B is very much similar to an edge-to-face style. This geometry describes the interaction between C-H of ring A and B and the edge of the ring B and A and vice-versa. In addition, interactions between the H-14 and C8=C7 olefinic bond and H-14 and C8=C7 olefinic bond are also observed for the alignment 5.2 originating from orientation 2. The distance between 12-OH and 5-OCH₃ or 12-OH and 5-OCH₃ is about 2.72 Å (Table 5.4 and 5.5). In addition, the measured distance between 12-OH and C-5 or 12-OH and C-5 is about 2.48 Å. These distances suggest the presence of weak hydrogen bonds.

In contrast, the alignment 5.5 originating from orientation 5 shows a strong hydrogen bond with a distance of 1.96 Å between 14-OH and 5-OCH₃ and a weak hydrogen bond between 12-OH/C-5 and 5-OCH₃ at a distance of 2.55 Å and 2.59 Å respectively. No interaction between olefinic and aromatic CH bonds was observed.

Geometry C

Geometry C can be considered as close to parallel displaced geometry with an offset of 1.4 Å. Apparently, the optimized alignment 5.3 obtained from orientation 3 remains in the parallel-displaced geometry of the parent orientation. In addition, there is an enhancement in the hydrogen bond strength between 12-OH/3-OCH₃ and 12-OH/3-OCH₃ with a distance of 1.97 Å (Table 5.4 and 5.5). For the alignment 5.4 that was obtained from optimization of orientation 4, it was observed that the ring A and B have shifted down by one carbon along y axis maintaining the parallel displaced geometry as above. This geometry also keeps intact the hydrogen bond between 12-OH/3-OCH₃ and 12-OH/3-OCH₃ at a distance of 1.97 Å.

Summary

Optimized alignments 5.1, 5.3 and 5.4 obtained from orientation 1, 3 and 4 favor parallel displaced geometry with stabilization energies of -11.63, -19.29 and -19.29 kcal/mol respectively. However, alignments 5.2 and 5.5 optimized from orientation 2 and 5 favor edge to face (CH- interaction) geometry with stabilization energies of -20.50 and -20.82 kcal/mol respectively. Clearly, alignment 5.1 has the highest stabilization energy due to the absence of hydrogen bonding. However, it seems that alignment 5.2 with no influence of hydrogen bond and alignment 5.5 with contribution from only one hydrogen bond have the lowest stabilizing energy compared to parallel displaced geometry with intact hydrogen bonds. Since the difference in the stabilization energy is very small, it is difficult to state the favored geometry. However, if the calculation is performed in presence of solvent, it would be possible to obtain the preferred geometry. From the above results, we can conclude that parallel displaced geometry is governed by hydrogen bond and π - π interactions, whereas edge-to-face geometry is governed by hydrogen bond and mainly CH- π interactions.

Table 5.4: Calculation results on various *Re/Si* approaches of pterostilbene units.

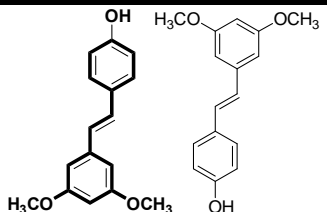
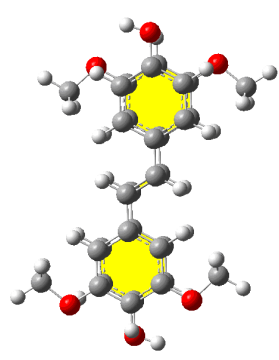
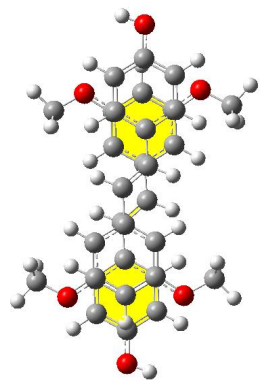
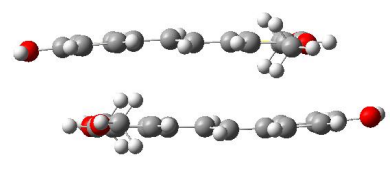
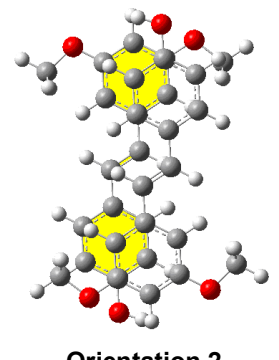
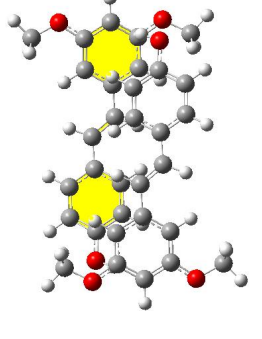
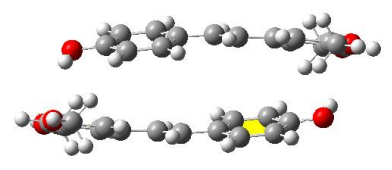
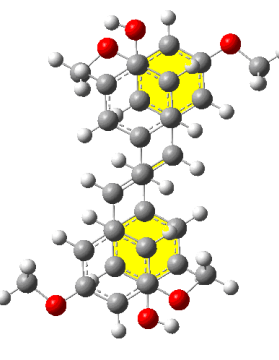
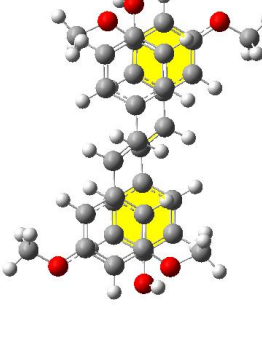
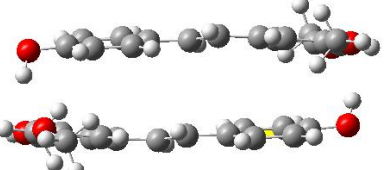
<div>  </div>		
Initial Orientation	Calculated geometry	
	Front view	Side view
<div>  </div> <p>Orientation 1</p>	<div>  </div> <p>Alignment 5.1 (Geometry A) -11.63 kcal/mol</p>	<div>  </div>
<div>  </div> <p>Orientation 2 C2ø in the middle of ring A</p>	<div>  </div> <p>Alignment 5.2 (Geometry B) -20.50 kcal/mol</p>	<div>  </div>
<div>  </div> <p>Orientation 3 C6ø in the middle of ring A</p>	<div>  </div> <p>Alignment 5.3 (Geometry C) -19.29 kcal/mol</p>	<div>  </div>

Table 5.6 (cont'd): Calculation results on various *Re/Re* approaches of pterostilbene units.

<p>Orientation 4 C5ø in the middle of ring A</p>	<p>Alignment 5.4 (Geometry C) -19.29 kcal/mol</p>	
<p>Orientation 5 C3ø in the middle of ring A</p>	<p>Alignment 5.5 (Geometry B) -20.82 kcal/mol</p>	

Table 5.5: Measured distances between selected atoms from alignment 5.1-5.5

	Alignment 5.1, Geometry A	Alignment 5.2, Geometry B	Alignment 5.3, Geometry C	Alignment 5.4, Geometry C	Alignment 5.5, Geometry B
12-OH/3'-OCH ₃ (Å)	4.40	4.35	1.97	1.97	4.27
12-OH/5'-OCH ₃ (Å)	5.04	2.72	4.89	4.89	2.59
12'-OH/5-OCH ₃ (Å)	5.09	2.71	4.89	4.89	1.96
12'-OH/3-OCH ₃ (Å)	4.34	4.34	1.97	1.96	5.58
C7/C7' (Å)	3.41	4.97	4.8	4.8	4.67
C7/C8' (Å)	3.65	4.88/4.88	3.91/3.91	3.92/3.92	4.92/4.74
HF stabilization (kcal/mol)	-11.63	-20.50	-19.29	-19.29	-20.82

5.5.4. Calculation results on various *Re/Re* approaches of pterostilbene units

Two pterostilbene units were aligned in a *Re/Re* manner at an inter-plane distance of 3.5 Å with the six different starting geometries (Table 5.6) listed below:

- i) face to face geometry (only ring B is placed on top of ring A): Orientation 7
- ii) Parallel displaced geometry with a C atom of ring B of a given unit is placed in the center of the ring A of the opposite unit as follows:
 - e) C-3 Orientation 6
 - f) C-2 Orientation 8
 - g) C-4 Orientation 9
 - h) C-5 Orientation 10
 - i) C-6 Orientation 11

The obtained optimized alignments can be categorized into two groups, geometries D and E.

Geometry D

Orientations 6, 7 and 8 gave geometry D where the stilbene units were aligned in edge-to-face styles. Optimized alignments 5.6 and 5.8 obtained from Orientation 6 and 8 have two hydrogen bonds each with stabilization energy of -20.46 kcal/mol and -20.76 kcal/mol respectively (Table 5.6). In contrast, the optimized alignment 5.7 obtained from Orientation 7 has one hydrogen bond and a weak interaction between 12-OH and C-5 of the aromatic ring at a distance of 2.42 Å with stabilization energy of -21.51 kcal/mol.

Geometry E

Orientations 9, 10 and 11 gave geometry E with the top and bottom rings being aligned in parallel displaced and edge-to-face styles respectively. All the three alignments (5.9, 5.10, and 5.11) have two hydrogen bonds each and identical stabilization energy of -21.33 kcal/mol (Table 5.6).

Table 5.6: Calculation results on various *Re/Re* approaches of pterostilbene units.

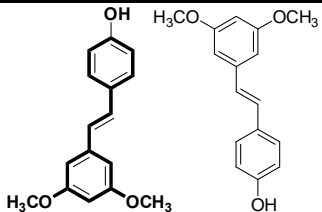
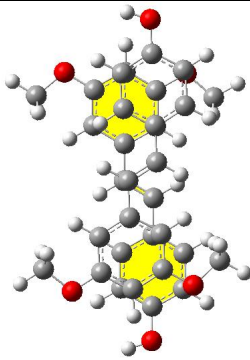
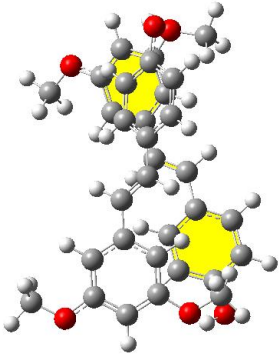
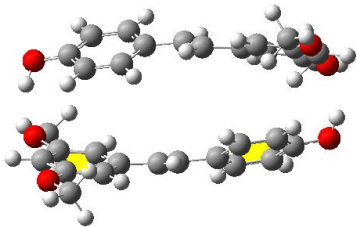
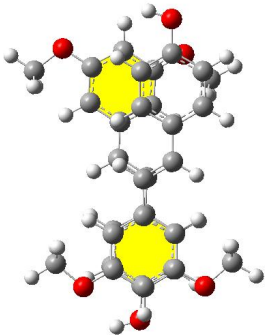
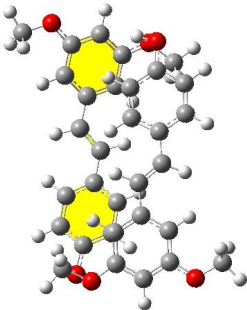
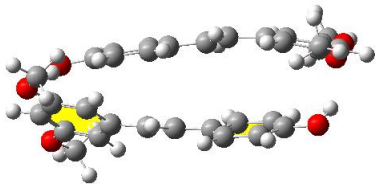
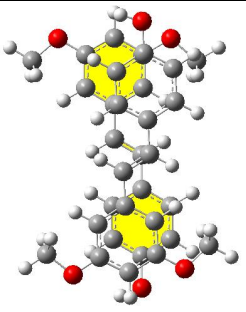
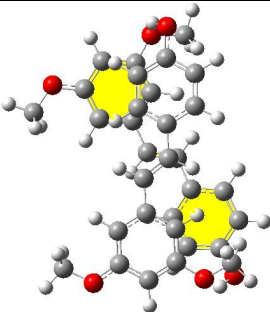
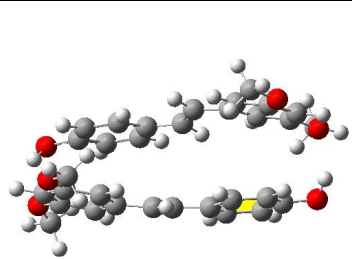
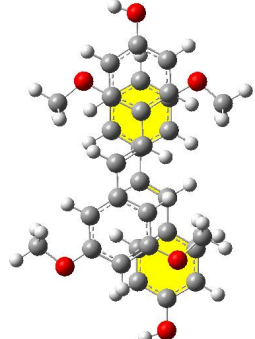
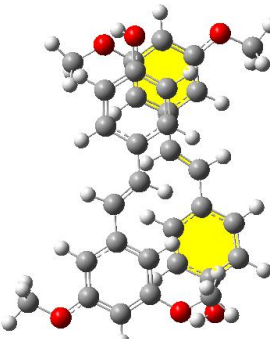
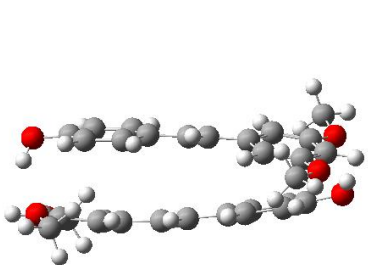
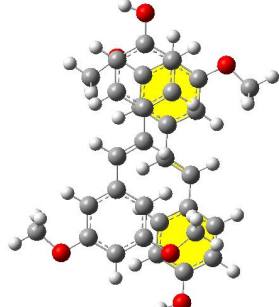
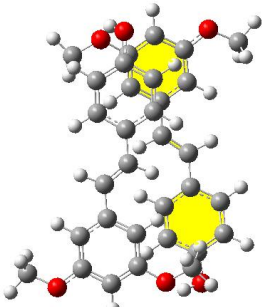
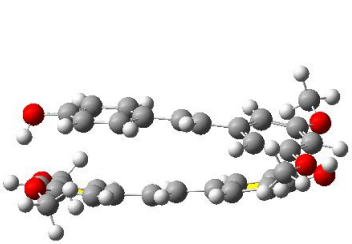
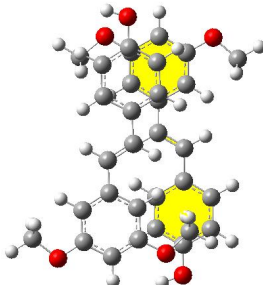
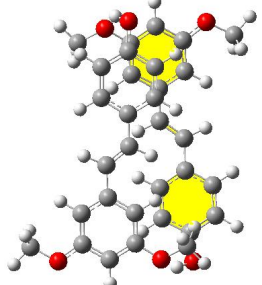
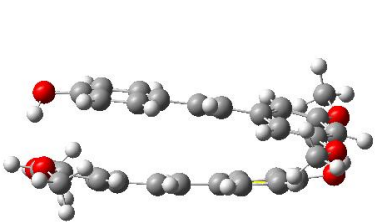
<div style="text-align: center;">  </div>		
Initial Orientation	Calculated Geometry	
	Front View	Side View
		
Orientation 6	Alignment 5.6 (Geometry D) -20.46 kcal/mol	
		
Orientation 7	Alignment 5.7 (Geometry D) -21.51 kcal/mol	

Table 5.6: Calculation results on various *Re/Re* approaches of pterostilbene units.

		
<p>Orientation 8</p>	<p>Alignment 5.8 (Geometry D) -20.76 kcal/mol</p>	
		
<p>Orientation 9</p>	<p>Alignment 5.9 (Geometry E) -21.33 kcal/mol</p>	
		
<p>Orientation 10</p>	<p>Alignment 5.10 (Geometry E) -21.33 kcal/mol</p>	
		
<p>Orientation 11</p>	<p>Alignment 5.11 (Geometry E) -21.33 kcal/mol</p>	

5.5.5. Calculation results on various *Re/Re* approaches of demethoxy-pterostilbene units with two methoxy groups aligned *syn* to each other

When two unsymmetrical molecules are aligned, we have to consider the positions of the substituents with respect to the longitudinal axis. In the case of the alignment of two units of demethoxypterostilbene (or 12-hydroxy-3-methoxystilbene) **5.3**, we shall use the term of *syn* when the two OCH₃ groups are located at the same side of the alignment, *anti* when they are on the opposite sides. Four different orientations that are similar to those used for calculations on pterostilbene in a *Re/Re* approach were employed. Due to this initial similarity they are named as orientations 6ø 7ø 10ø and 11ø (Table 5.7). All the four optimized arrangements can be classified as edge-to-face (Geometry F) when the two methoxy groups from the stilbene units were aligned *syn* to each other. Optimized alignments 5.13 and 5.15 originated from Orientations 7ø and 11ø have one hydrogen bond. Alignment 5.12 has a weak hydrogen bond between 12-OH and C6ø=C5ø of the aromatic ring. Alignment 5.14 does not allow any hydrogen bond. Stabilization energies for optimized alignments from orientations 6ø 7ø 10ø and 11ø are -16.48, -17.24, -17.11 and -17.24 kcal/mol respectively.

Table 5.7: Calculation results on various *Re/Re* approaches of demethoxypterostilbene units with two methoxy groups aligned *syn* to each other.

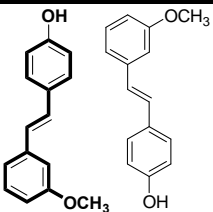
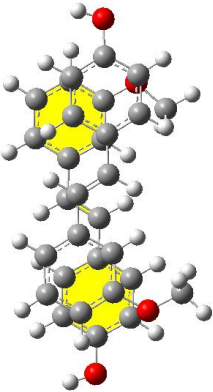
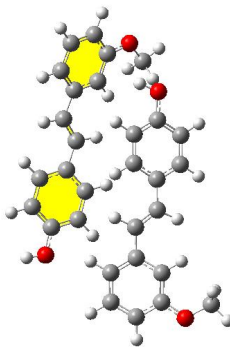
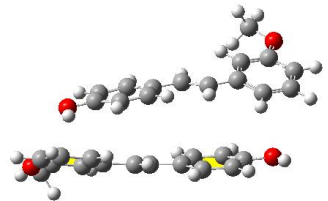
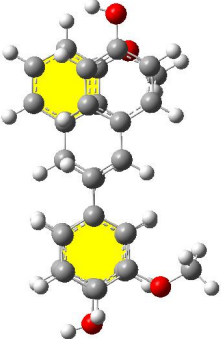
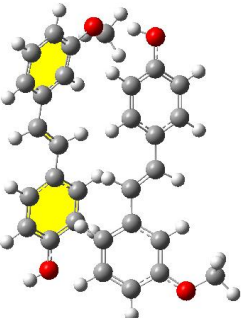
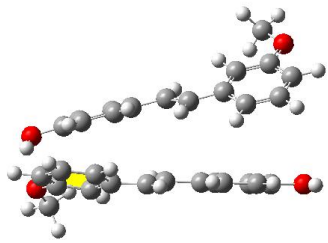
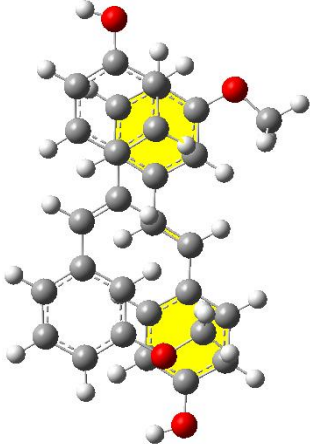
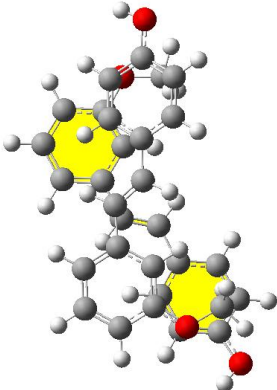
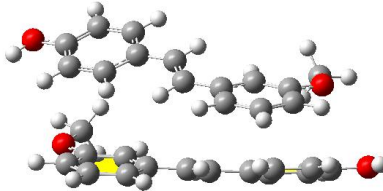
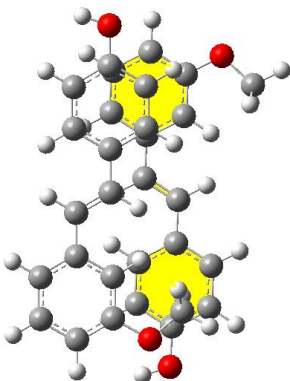
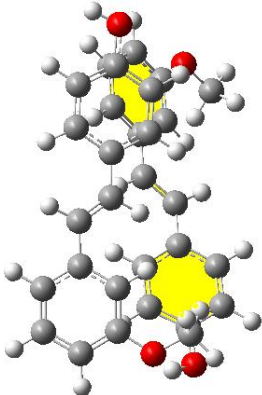
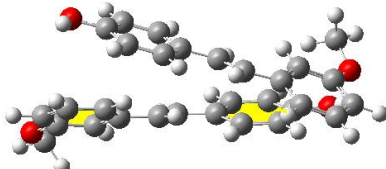
<div>  </div>		
Initial Orientation	Calculated geometry	
	Front View	Side View
		
Orientation 6ø	Alignment 5.12 (Geometry F) -16.48 kcal/mol	
		
Orientation 7ø	Alignment 5.13 (Geometry F) -17.24 kcal/mol	

Table 5.7 (cont'd): Calculation results on various *Re/Re* approaches of demethoxypterostilbene units with two methoxy groups aligned *syn* to each other.

		
Orientation 10ø	Alignment 5.14 (Geometry F) -17.11 kcal/mol	
		
Orientation 11ø	Alignment 5.15 (Geometry F) -17.24 kcal/mol	

5.5.6. Calculation results on various *Re/Re* approaches of demethoxy-pterostilbene units with two methoxy groups aligned *anti* to each other

Five different orientations (Orientations 6øø, 7øø, 8øø, 10øø and 11øø) as described in section 5.5.5 were employed for *Re/Re* alignment of demethoxypterostilbene units (Table 5.8). The two methoxy groups from the stilbene

units were aligned *anti* to each other. The obtained optimized alignments can be categorized into two groups, Geometries G and H.

Geometry G

Orientations 6 $\emptyset\emptyset$, 10 $\emptyset\emptyset$ and 11 $\emptyset\emptyset$ gave Geometry D, where the stilbene units are aligned in edge-to-face style. Optimized alignments 5.16 and 5.20 obtained from Orientations 6 $\emptyset\emptyset$ and 11 $\emptyset\emptyset$ show the presence of weak interactions between 12-OH and C-3 \emptyset 12 \emptyset -OH and C-3 of the aromatic rings at a distance of 2.3 Å with stabilization energy of -18.34 kcal/mol and -14.72 kcal/mol respectively (Table 5.8). However, optimized alignment 5.19 obtained from Orientation 10 $\emptyset\emptyset$ has one hydrogen bond with stabilization energy of -16.15 kcal/mol.

Geometry H

Orientations 7 $\emptyset\emptyset$ and 8 $\emptyset\emptyset$ gave geometry E after calculations; the top and bottom rings were aligned in edge-to-face and parallel displaced styles respectively. Both alignments have two hydrogen bonds each and identical stabilization energy of -21.31 kcal/mol (Table 5.8).

Table 5.8: Calculation results on various *Re/Re* approaches of demethoxypterostilbene units with two methoxy groups aligned anti to each other.

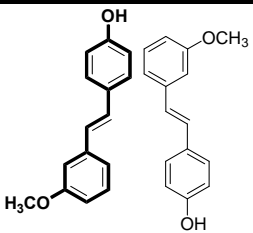
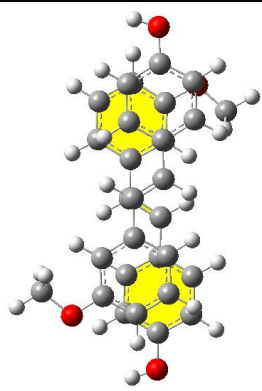
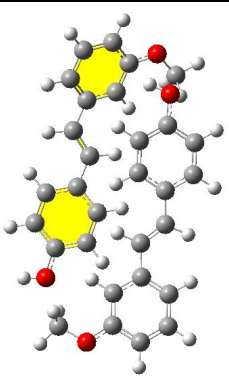
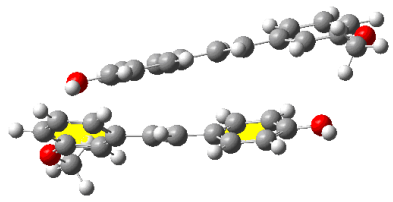
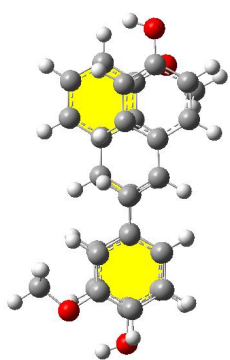
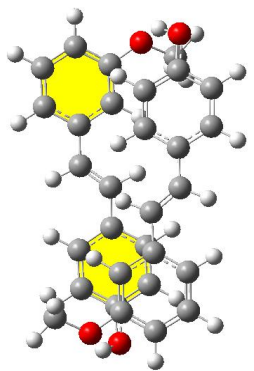
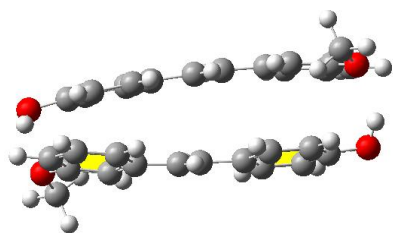
<div style="text-align: center;">  </div>		
Initial Orientation	Calculated Geometry	
	Front View	Side View
		
Orientation 6''	Alignment 5.16 (Geometry G) -18.34 kcal/mol	
		
Orientation 7''	Alignment 5.17 (Geometry H) -21.31 kcal/mol	

Table 5.8: Calculation results on various *Re/Re* approaches of demethoxypterostilbene units with two methoxy groups aligned anti to each other.

Orientation 8''	Alignment 5.18 (Geometry H) -21.31 kcal/mol	
Orientation 10''	Alignment 5.19 (Geometry G) -16.15 kcal/mol	
Orientation 11''	Alignment 5.20 (Geometry G) -14.72 kcal/mol	

5.5.7. Calculation results on various *Re/Si* approaches of demethoxy-pterostilbene units with two methoxy groups were aligned *anti* to each other

Four different orientations that are similar to those used for calculations on pterostilbene in *Re/Si* approach were employed. Due to this initial similarity they are named as orientations 2ø, 3ø, 4ø and 5ø (Table 5.9). The two methoxy groups from the stilbene units were aligned *anti* to each other. The obtained optimized alignments can be categorized into two groups, Geometry I and J.

Geometry I

Orientations 2ø and 5ø gave geometry I where the stilbene units were aligned in edge-to-face styles. Optimized alignment 5.21 obtained from Orientation 2ø show weak interactions between 12ø-OH and C-6/12-OH and C-6ø of aromatic rings with stabilization energy of -20.74 kcal/mol (Table 5.9). However, the optimized alignment 5.24 obtained from Orientation 5ø displays one hydrogen bond with stabilization energy of -20.32 kcal/mol.

Geometry J

Orientations 3ø and 4ø gave geometry J, aligned in parallel displaced manner with stabilization energies of -9.55 kcal/mol and -8.53 kcal/mol respectively (Table 5.9). Both the optimized alignments 5.22 and 5.23 have no influence of hydrogen bond.

Table 5.9: Calculation results on various *Re/Si* approaches of demethoxypterostilbene units with two methoxy groups aligned anti to each other

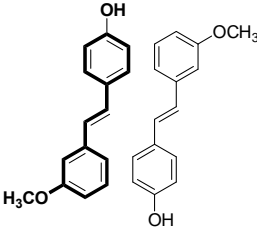
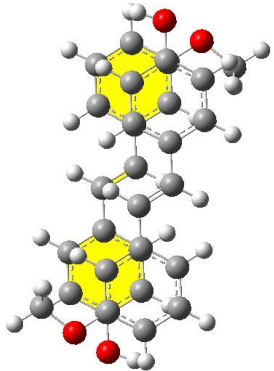
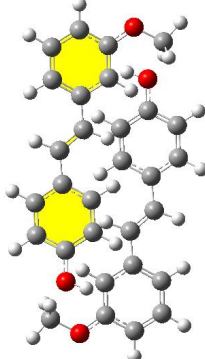
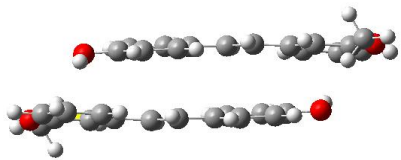
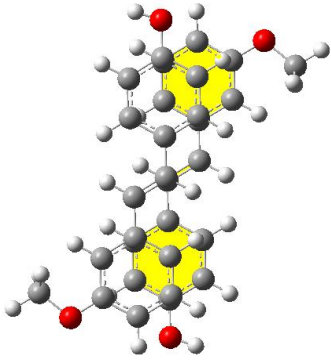
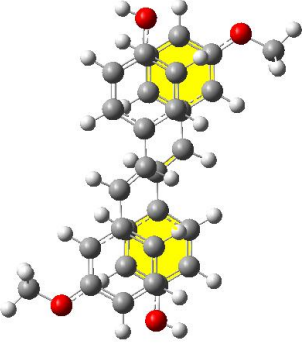
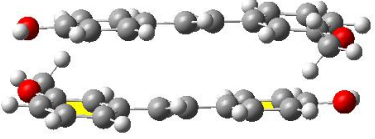
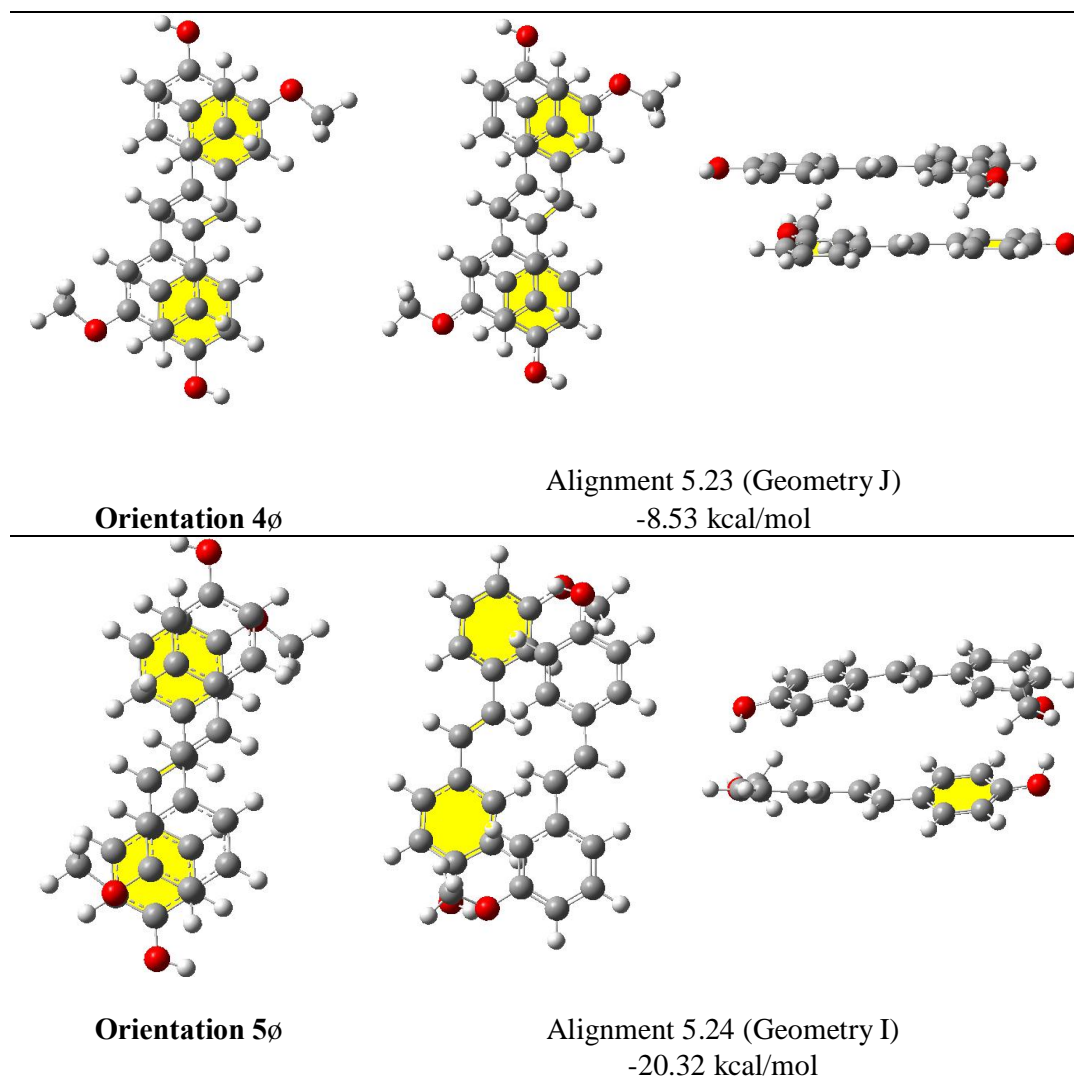
<div style="text-align: center;">  </div>		
Initial Orientation	Calculated Geometry	
	Front View	Side View
		
Orientation 2'	Alignment 5.21 (Geometry I) -20.74 kcal/mol	
		
Orientation 3ø	Alignment 5.22 (Geometry J) -9.55 kcal/mol	

Table 5.9 (cont'd): Calculation results on various *Re/Si* approaches of demethoxypterostilbene units with two methoxy groups aligned anti to each other



5.5.8. Summary

Re/Si approaches of pterostilbene units gave three alignments (Geometries A, B and C in Table 5.4) where two of them are arranged in parallel displaced manner and the other in edge-to-face style. It appears that there is not much difference in energy between geometries B and C ranging from -19 to -21 kcal/mol. These geometries are stabilized by both π interaction and H bond. Due to the absence of H bond, geometry A can be ruled out since it has the highest energy of -11.6 kcal/mol.

Therefore, geometry B (edge-to-face) and C (parallel displaced) can be considered as the major possible geometries for *Re/Si* approaches of pterostilbene units.

Re/Re approaches of pterostilbene units produce two types of alignments (Geometries D and E in Table 5.6) in edge-to-face style and combination of parallel displaced and edge-to-face manner, respectively. Their stabilizing energies vary from -20.0 to -20.5 kcal/mol. Since there is no big difference in their stabilization energies of Geometries D and E, could be the preferred geometries for *Re/Re* approaches of pterostilbene units.

Four similar alignments collectively called Geometry F were obtained when demethoxypterostilbene units were aligned in *Re/Re* manner with the methoxy groups of the stilbene units *syn* to each other. They are edge-to-face arrangements with stabilization energy ranging between -16 to -17 kcal/mol. When the methoxy groups of the stilbene units were *anti* to each other, three alignments (Geometry G) were obtained in edge-to-face style (Geometry H, 14 to 18 kcal/mol) and the other two in combination of parallel displaced and edge-to-face manner (-21.3 kcal/mol). Geometry F and G can be ruled out as the rings are distorted and possess lower stabilization energy. This has left us with Geometry H as the probable geometry for *Re/Re* approaches of demethoxypterostilbene units with methoxy groups being *anti* to each other.

Re/Si approaches of demethoxypterostilbene units with methoxy groups *anti* to each other gave Geometry I, edge-to-face style and J, parallel displaced. Geometry I has stabilization energy around 21.0 kcal/mol whereas Geometry J around 9.0 kcal/mol. The high difference of 10 kcal/mol in stabilization energy between Geometry I and J is explained by the absence of hydrogen bonds which are important contributors to the stabilization of the parallel displaced alignment.

5.5.9. Study of oxidized stilbene species and their reactivities

To provide a better understanding of stilbene dimerisation and the formation of intermediates **4.208** (Scheme 4.65, Chapter 4), **4.210** (Scheme 4.65, Chapter 4) and **4.216** (Scheme 4.70, Chapter 4) leading to the formation of ampelopsin F, pallidol and tetralin type analogues, one can imagine that in solution one of the previously described complexes is formed. From this complex either one or two stilbene unit(s) is(are) oxidized. In the case of stilbene derivatives, a hydrogen atom is removed from 12-OH group from one (or two) of the stilbenes. This step corresponds to the oxidative reaction that may occur on the most active group (lower BDE). In the former case (one H atom is removed) the pair now comprising one native stilbene and one radical stilbene. A new round of calculations can then be achieved. In the latter case (both stilbene units are oxidized) the pair now consists of two radical stilbenes, which were then subjected to calculation as well. The new calculations of the oxidized complexes will provide sensible hypothesis on the favored alignments of stilbenoid species that allow the formation of the dimers observed experimentally.

5.5.9.1. Pterostilbene/pterostilbene radical

From the study on the alignment of pterostilbene units resulting from *Re/Si* approaches (section 5.5.3), only orientations leading to Geometries B and C were considered as the latter have similar and low stabilization energy for the formation of intermediate **4.208**.

H^E removal out of one of the stilbene units from Orientations 5 and 3 and subsequent calculation led to alignments 5.25 and 5.26 respectively (Figure 5.18). Alignment 5.25 shows a greater displacement along *y* axis as compared to alignment 5.5, with $C7/C8 = 5.85 \text{ \AA}$ and $C7/C7 = 6.10 \text{ \AA}$. As a result it cannot be considered as a

reliable model. By contrast, alignment 5.26 is very similar with alignment 5.3 or 5.4. The distances between C7 and C7 ϕ and C8 are reduced to 4.66 Å and 3.84 Å respectively. These distances are probably too large to allow spontaneous C7/C7 ϕ or C7/C8 ϕ bond formation but show an activation of the stilbene pair. [These reduced distances would allow spontaneous bond formation even though the stabilization energy is higher than alignment 5.25 by 3.05 kcal/mol.] See also Chapter 4, Scheme 4.65.

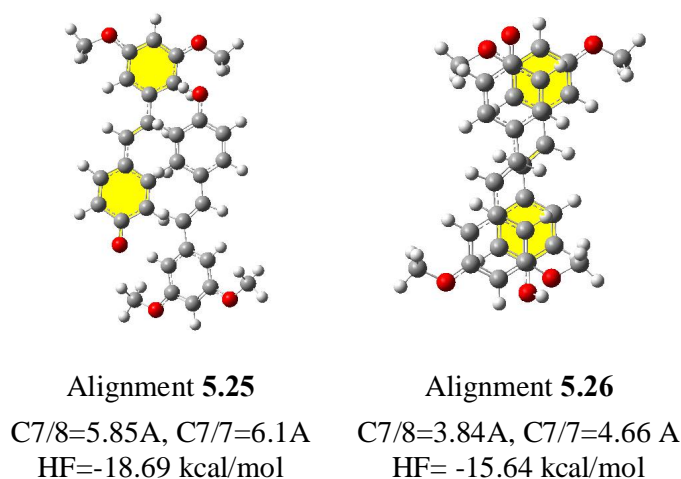


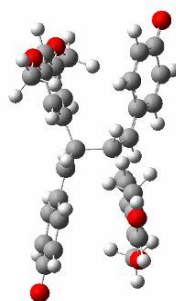
Figure 5.18: Calculation results on *Re/Si* approaches of pterostilbene-pterostilbene radical.

5.5.9.2. Pterostilbene radical/pterostilbene radical

From the study on the alignment of pterostilbene units resulting from *Re/Re* approaches (section 5.5.4), orientations leading to geometries D and E were considered as they have similar stabilization energy for the formation of intermediate **4.210**.

Removal of two H atoms from two stilbene units from Orientation 11 and subsequent calculation led to intermediate **5.10** with stabilization energy of -30.42 kcal/mol (Figure 5.19). **5.10** shows bond formation between C7 and C7 ϕ due to high spin density at both the C7 and C7 ϕ . However, this was not the case when the two

stilbene radicals were aligned in a *Re/Si* manner. As a result, this suggests that the formation of intermediate **4.210** (Scheme 4.65, Chapter 4) has to undergo *Re/Re* approaches by two stilbene radicals.



Intermediate **5.10**
HF=-30.42 kcal/mol

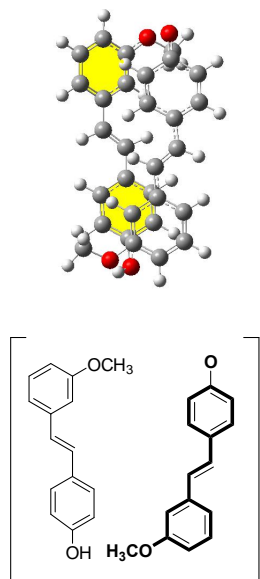
Figure 5.19: Calculation result on *Re/Re* approaches of pterostilbene radical-pterostilbene radical.

5.5.9.3. Demethoxy-pterostilbene/demethoxy-pterostilbene radical

From the study on the alignment of demethoxypterostilbene units resulting from *Re/Re* approaches (section 5.5.5 and 5.5.6), only orientation leading to Geometry H was considered for the formation of intermediate **4.216** as it has the lowest stabilization energy. H^E removal out of one of the stilbene units from Orientations 7ö or 8ö and subsequent calculation led to alignment 5.28 (Figure 5.20).

Alignment 5.28 (stabilization energy = -16.53 kcal/mol) shows a similar arrangement as shown in alignment 5.18 but now, just one hydrogen bond is been established with C7/C8ö = 3.63 Å and C7/C7ö=4.29 Å. Stabilization energy of alignment 5.28 is -16.53 kcal/mol higher than the stilbene alignment 5.18 (21.31 kcal/mol) originated from orientation 8ö indicating a reactive stilbene pair is been formed. Since the distance between C7 and C8ö is shorter than the distance between C7 and C7ö a spontaneous bond formation can be expected between C7 and C8ö (Chapter, Scheme 4.70).

In addition, *Re/Si* approaches of demethoxypterostilbene-demethoxypterostilbene radical were not considered as the alignments of native pair (demethoxypterostilbene- demethoxypterostilbene) are collectively the least stable arrangements. This could explain why there is no product formation from *Re/Si* approaches in the ferric chloride oxidative coupling reaction of demethoxypterostilbene (Chapter, Scheme 4.70).



Alignment 5.28
 $C7/8 = 3.63\text{\AA}$, $C7/7 = 4.29\text{\AA}$
 $HF = -16.53\text{ kcal/mol}$

Figure 5.20: Calculation result on *Re/Re* approaches of demethoxypterostilbene-demethoxypterostilbene radical.

5.5.9.4. Demethoxy-pterostilbene radical/demethoxy-pterostilbene radical

As described above for the alignment of demethoxypterostilbene units resulting from *Re/Re* approaches, removal of two H atoms from the stilbene units from Orientation 7ö and subsequent calculation led to **5.11** (Figure 5.21). Species **5.11** shows bond formation between C7 and C7ø with stabilization energy of -28.8 kcal/mol (Figure 5.21).

The fact that no product was obtained with C7/7 ϕ bond in the ferric chloride oxidative coupling of demethoxypterostilbene (Chapter 4, Scheme 4.70) would possibly explain that this reaction might be kinetically driven, whereas in the case of *Re/Re* approaches of two pterostilbene radicals, formation of intermediate **4.210** with C7/C7 ϕ bond could be led thermodynamically. Anyhow, to confirm this idea, more calculations would need to be carried out.

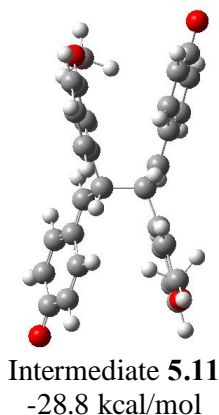


Figure 5.21: Calculation result on *Re/Re* approaches of demethoxypterostilbene radical- demethoxypterostilbene radical.

5.6. Ag⁺ impact on its coordination with stilbene and the alignment of stilbenes

As described in Chapter 4, section 4.3.5.6, herein the coordination of Ag⁺ with stilbene is successfully modelled to support the previously proposed idea, obtaining the optimized conformation of stilbene-Ag⁺ complex (Figure 5.22).

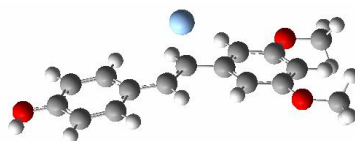


Figure 5.22: Stilbene-Ag⁺ model.

Below are the examples of lowest unoccupied molecular orbital (LUMO) and highest occupied molecular orbitals (HOMO, HOMO-1 and HOMO-2) (Figure 5.23) which correspond to stilbene- Ag^+ complex. HOMO-2 clearly shows the d orbital of the Ag^+ ion involved in the complication.

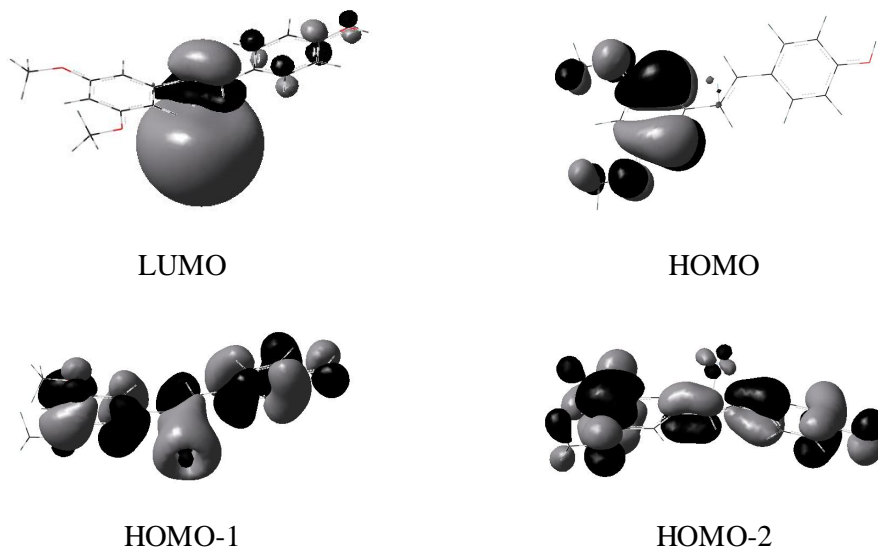


Figure 5.23: LUMO, HOMO, HOMO-1 and HOMO-2 of stilbene- Ag^+ complex.

Since Ag^+ coordinate well with the olefinic bond of stilbene, thus has inspired us to study what will be the metal ion impact on two stilbenes in a stack. Any species (example: stilbene) having π - π interactions aligned in a stack should held both the species together at a distance of 3.77 \AA (Figure 5.24). To test this known principle to the above stilbene- Ag^+ complex, another stilbene was laid on top of this complex at the distance of 3.77 \AA and was submitted for calculation. Interestingly, the result showed that the calculated distance is 5.34 \AA , 1.57 \AA larger than the standard distance (Figure 5.24).

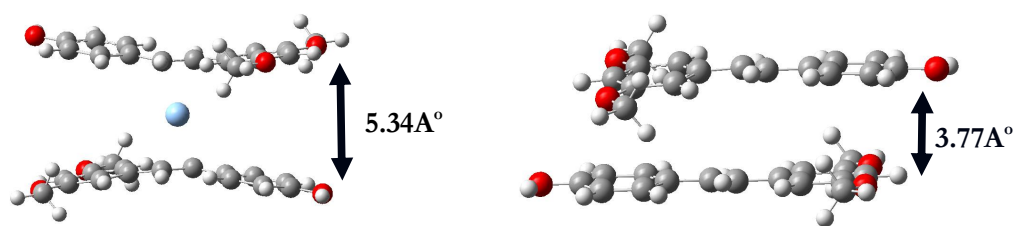


Figure 5.24: Calculated distance between stack of stilbenoids with and without Ag^+ .

This indicates that the stilbenes stack, which is held by π - π interactions is destroyed by the presence of bulky Ag^+ ion. Possibly, free stilbenes are generated, which then direct them to approach each other in a T-shape manner as described in previous Chapter 4, section.4.3.5.6, thus reinforcing the proposed idea.

In summary, calculations show that planar neutral stilbenes can be stacked and the two important interactions that hold this stack are π - π interactions and hydrogen bonding. Two different types of geometries are observed generally, edge-to-face and parallel displaced with both type of alignments having the lowest energy in most cases. Perhaps, the selectivity of the preferred alignment is possibly to be obtained if the calculations are done in the presence of solvent. It is also observed that the presence of metal ions in the stack could also destroy the non covalent interactions between two stilbenes. The calculation of alignments consisting two stilbene radicals, immediately lead to the formation of intermediate with lowest energy. The interlinkage bond between two stilbenes in the intermediate is established at the highest distribution of spin densities over the stilbenes.

5.7. References

1. E. V. Anslyn, D. A. Dougherty, *Modern Physical Organic Chemistry*, University Science Books, Sausalito, California, 2004.
2. J. W. Steed, J. L. Atwood, *Supramolecular Chemistry*, John Wiley & Sons, Ltd, 2000.
3. L. M. Raff, *Principles of Physical Chemistry*, Prentice Hall, Upper Saddle River, NJ 07458, 2001.
4. I. N. Levine, *Physical Chemistry*, 5th ed, Mc Graw Hill, 2002.
5. (a) F. Jensen, *Introduction to Computational Chemistry*, 2nd ed, John Wiley & Sons, Ltd, West Susses, England, 2007.

(b) Gaussian 03, M. J. Frisch, G. W. Trucks, H. B. Schlegel, G. E. Scuseria, M. A. Rob, J. R. Cheeseman, J. A. Montgomery Jr., T. Vreven, K. N. Kudin, J. C. Burant, J. M. Millam, S. S. Iyengar, J. Tomasi, V. Barone, B. Mennucci, M. Cossi, G. Scalmani, N. Rega, G. A. Petersson, H. Nakatsuji, M. Hada, M. Ehara, K. Toyota, R. Fukuda, J. Hasegawa, M. Ishida, T. Nakajima, Y. Honda, O. Kitao, H. Nakai, M. Klene, X. Li, J. E. Knox, H. P. Hratchian, J. B. Cross, V. Bakken, C. Adamo, J. Jaramillo, R. Gomperts, R. E. Stratmann, O. Yazyev, A. J. Austin, R. Cammi, C. Pomelli, J. W. Ochterski, P. Y. Ayala, K. Morokuma, G. A. Voth, P. Salvador, J. J. Dannenberg, V. G. Zakrzewski, S. Dapprich, A. D. Daniels, M. C. Strain, O. Farkas, D. K. Malick, A. D. Rabuck, K. Raghavachari, J. B. Foresman, J. V. Ortiz, Q. Cui, A. G. Baboul, S. Clifford, J. Cioslowski, B. B. Stefanov, G. Liu, A. Liashenko, P. Piskorz, I. Komaromi, R. L. Martin, D. J. Fox, T. Keith, M. A. Al-Laham, C. Y. Peng, A. Nanayakkara, M. Challacombe,

- P. M. W. Gill, B. Johnson, W. Chen, M. W. Wong, C. Gonzalez, J. A. Pople, Gaussian, Inc., Wallingford, CT, 2003.
6. E. A. Meyer, R. K. Castellano, F. Diederich, *Angew. Chem. Int. Ed.*, 2003, **42**, 1210-1249.
 7. Z.-T. Zhang, X.-B. Wang, Q.-Y. Wang, L.-N. Wu, *J. Chem. Crystallogr.*, 2005, **35**, 923-929.
 8. C. A. Hunter, K. R. Lawson, J. Perkins, C. J. Urch, *J. Chem. Soc., Perkin Trans. 2*, 2001, 651-669.
 9. C. A. Hunter, J. K. M. Sanders, *J. Am. Chem. Soc.*, 1990, **112**, 5525-5534.
 10. B. W. Gung, J. C. Amicangelo, *J. Org. Chem.*, 2006, **71**, 9261-9270.
 11. a) M. I. Burguete, M. Bolte, J. C. Frias, E. G.-Espana, S. V. Luis, J. F. Miravet, *Tetrahedron*, 2002, **58**, 4179-4183. b) Z.-T. Zhang, X.-L. Zhang, *J. Chem. Crystallogr.*, 2008, **38**, 129-133.
 12. S. K. Burley, G. A. Petsko, *Science*, 1985, **229**, 23.
 13. G. W. Coates, A. R. Dunn, L. M. Henling, D. A. Dougherty, R. H. Grubbs, *Angew. Chem., Int. Ed. Eng.*, 1997, **36**, 248-251.
 14. H.-Y. Zhang, Y.-M. Sun, D.-Z. Chen, *Quant. Struct.-Act. Relat.*, 2001, **20**, 148-152.
 15. D. Kozlowski, P. Trouillas, C. Calliste; P. Marsal, R. Lazzaroni, J. L. Duroux, *J. Phys. Chem. A*, 2007, **111**, 1138.
 16. E. Anouar, C. A. Calliste, P. Kosinova, F. Di Meo, J. L. Duroux, Y. Champavier, K. Marakchi, P. Trouillas, *J. Phys. Chem. A*, 2009, **113**, 13881-13891.
 17. P. Trouillas, P. Marsal, D. Siri, R. Lazzaroni, J. L. Duroux, *Food Chem.*, 2006, **97**, 679.

18. H. Cao, X. Pan, C. Li, C. Zhou, F. Deng, T. Li, *Bioorg. Med. Chem. Lett.*, 2003, **13**, 1869-1871.
19. M. P. Waller, A. Robertazzi, J. A. Platts, D. E. Hibbs, P. A. Williams, *J. Comput. Chem.*, 2006, **27**, 491-504.